

## REVIEW

[View Article Online](#)  
[View Journal](#)

Cite this: DOI: 10.1039/d5ta06598d

## Recent advances in MXene-based self-powered electrochemical sensors

Ajith Mohan Arjun, <sup>a</sup> Menon Ankitha, <sup>b</sup> Manjusha Mathew, <sup>c</sup> Sanjiv Sharma <sup>a</sup> and P. Abdul Rasheed <sup>\*db</sup>

Self-powered electrochemical sensors (SPECs) offer a transformative alternative by integrating energy harvesting directly with analyte detection, enabling autonomous operation without external power sources. This review focuses on the merits of employing MXenes in the construction and performance of SPECs by evaluating how MXenes are employed as active components and how they enhance the performance of various SPECs platforms. We broadly classified MXene-based SPECs as enzymatic biofuel cell-based sensors, microbial- and biophotoelectrochemical-based sensors, and other SPECs. The key attributes of MXenes, including high conductivity and tunable surface chemistry, are ideal for immobilizing active species in the SPECs. The significant capacitance and catalytic potential of MXenes are explored towards enhancing charge transport in SPECs. This enables robust interfaces, facilitating

Received 14th August 2025  
Accepted 10th November 2025

DOI: 10.1039/d5ta06598d

[rsc.li/materials-a](https://rsc.li/materials-a)

<sup>a</sup>Department of Pharmacy and Therapeutics, Institute of Systems, Molecular and Integrative Biology, University of Liverpool, 6 W Derby St., Liverpool L7 8TX, UK. E-mail: [arjun.mohan@liverpool.ac.uk](mailto:arjun.mohan@liverpool.ac.uk); [Sanjiv.Sharma@liverpool.ac.uk](mailto:Sanjiv.Sharma@liverpool.ac.uk)

<sup>b</sup>Department of Chemistry, Indian Institute of Technology Palakkad, Palakkad, Kerala 678 623, India. E-mail: [abdulrasheed@iitpkd.ac.in](mailto:abdulrasheed@iitpkd.ac.in)

<sup>c</sup>Department of Chemistry, Nirmalagiri College, Kuthuparamba, Kannur, Kerala, 670701, India

<sup>d</sup>Department of Biological Sciences and Engineering, Indian Institute of Technology Palakkad, Palakkad, Kerala 678 623, India



Ajith Mohan Arjun

Ajith Mohan Arjun is an R&D Scientist specializing in advanced nanomaterials and electrochemical sensing platforms for diagnostics. Following his PhD in Materials Science and Engineering from the National Institute of Technology Calicut, India, he completed post-doctoral research at the University of Virginia and Indian Institute of Technology Palakkad, on aptamer based electrochemical sensors and applications of

MXene-based composites, respectively. As an MRC-AMED Research Fellow at the University of Liverpool (2023–2024), he developed microneedle-based sensors for ISF analysis and innovated point-of-care devices for neurological diagnosis, including Alzheimer's disease. Currently, as a Development Scientist in industry he leads projects focused on commercializing advanced diagnostic technologies, specifically developing immunoassays for monitoring women's health and enzymatic sensors for ketone and glucose metabolite analysis, leveraging his core expertise in wearable sensors and POC diagnostics. His research interests include electrochemical biosensors, enzymatic fuel cells, and wearable electrochemical sensors which involve the use of nanomaterials.



Menon Ankitha

Menon Ankitha is a Prime Minister's Research Fellow at the Indian Institute of Technology (IIT) Palakkad, India. She obtained her Master's degree in Chemistry from Sree Sankara College, Kalady, under Mahatma Gandhi University, where she ranked first in her class. Her research primarily focuses on the development of miniaturized, low-cost electrochemical sensors for real-time detection of biomarkers and

drug molecules. She specializes in integrating MXene-based hybrid nanomaterials with flexible substrates to develop wearable and point-of-care diagnostic devices.



signal amplification, and forming advanced functional composites within these self-powered devices. By utilizing these unique properties of MXenes, the development of highly sensitive, stable, and potentially miniaturized autonomous sensors is becoming increasingly feasible, paving the way for next-generation sensing solutions.

## 1. Introduction

Electrochemical sensors are essential tools, playing a pivotal role across diverse fields, including environmental monitoring, healthcare, food industry, agriculture, safety and security, and biotechnology research. A key operational requirement for conventional electrochemical sensors, despite their widespread utility, is their reliance on external power sources like batteries (for portable devices) or mains electricity (for stationary systems). This fundamental dependency on external power introduces significant limitations concerning device self-sufficiency, overall sustainability, system resilience, maintenance logistics, and environmental impact. To overcome these

challenges, self-powered electrochemical sensors (SPECSS) represent a transformative approach and a significant evolution in sensor technology.<sup>1,2</sup> These SPECSS operate by generating the electrical energy autonomously. This energy generation occurs through a process where the power output is directly controlled by the presence and concentration of the target analyte.<sup>3</sup> This integration of *in situ* power generation with sensing represents a paradigm shift towards more sustainable, autonomous, and simplified sensing platforms, which leads to the development of next-generation devices.

The autonomous generation of power in SPECSS directly addresses the significant sustainability challenges posed by conventional sensors. By eliminating the need for external power sources like batteries or solar cells, SPECSS drastically reduce the overall material usage involved in sensor construction. This not only conserves resources but also frees up valuable materials, including precious metals and rare earth elements used in batteries, for other critical applications. Furthermore, many SPECSS, particularly those based on biofuel cells, utilize biomaterials like enzymes and microbes that are more abundant and less environmentally intensive to produce than the components of traditional power sources.<sup>4</sup> This reduction in the reliance on resource-intensive, non-renewable materials directly results in a smaller carbon footprint and a more sustainable, self-sufficient sensing platform. This shift marks a move toward a circular economy model for sensors, where the device's operational power is seamlessly integrated with its sensing function, minimizing waste and environmental impact from cradle to grave.



Manjusha Mathew

*Manjusha Mathew received her PhD from the National Institute of Technology Calicut, India, in 2014. She has been serving as an Assistant Professor in the Department of Chemistry at Nirmalagiri College, Kuthuparamba, Kerala, India, since 2013. Her research interests include the development of electrochemical sensors and the design and application of nano-materials for energy storage.*



Sanjiv Sharma

*Sanjiv Sharma is a Senior Lecturer in Infectious Diseases and Antimicrobial Resistance at the University of Liverpool, where he leads the Smart Sensors Research Group. His research focuses on the design and development of low-cost electrochemical biosensing technologies for real-time monitoring of metabolites, drugs, and disease biomarkers across One Health (human and veterinary) settings. He has authored more*

*than 85 publications and has secured over £3 million in research funding. Dr Sharma is a Fellow of the Royal Society of Chemistry and the Higher Education Academy and is both a Chartered Scientist and a Chartered Chemist.*



P. Abdul Rasheed

*P. Abdul Rasheed received his PhD Degree from the School of Nano Science and Technology at National Institute of Technology Calicut, India in 2015. After his PhD, He did his postdoctoral fellowships at Korea University, South Korea, and in Qatar Environment and Energy research Institute, Doha, Qatar. He has received the prestigious Ramalingaswami Re-entry fellowship from the Department of Biotechnology, Government of*

*India, in 2021. Currently, he is a Ramalingaswami Fellow in the Department of Biological Sciences and Engineering at the Indian Institute of Technology Palakkad, India. His research interests are MXenes and other 2D materials, nanomaterial-based biosensors, wearable sensors, biomarkers for neurological disorders, and biomedical engineering.*



This paradigm shift towards SPEC systems needs to have innovative device designs that are capable of harvesting energy directly from their surroundings or from the electrochemical sensing reaction happening in the system itself. This can be realized by introducing diverse energy conversion strategies integrated directly within the sensor design. The key approaches include (1) harnessing biomechanical energy by using piezoelectric or triboelectric effects to convert vibrations or pressure changes,<sup>5</sup> (2) exploiting biochemical reactions similar to enzymatic biofuel cells, where analyte consumption generates current,<sup>2</sup> (3) utilizing thermal gradients *via* thermoelectric generators,<sup>6</sup> (4) capturing ambient light through photovoltaic components,<sup>7</sup> and (5) converting chemical potential directly into electricity.<sup>8</sup> The crucial aspects of design, operation, and potential applications of the sensor are entirely dependent on the selection of the energy harvesting mechanism used in the sensor system. For example, a wearable sensor can utilize the body movement *via* triboelectric nanogenerators, while an environmental sensor can utilize a biofuel cell powered by pollutants.<sup>9</sup> Hence, the sensor design should focus on analyte detection and efficient power generation units in addition to the integration of sensing elements with miniaturized, and operational demands of the sensor.

There are mainly two different approaches such as biofuel cells (BFCs) and photoelectrochemical (PEC) reactions, generally utilized in self-powered electrochemical sensing systems. These systems align with biological and environmental monitoring needs in a way that they generate power directly from metabolites readily available in physiological fluids (like glucose or lactate) in the case of BFCs, or by converting the light energy into PEC systems. A BFC-based self-powered system involves designing a fuel cell electrode with a primary biocatalyst for power generation, and a bioreceptor element that undergoes bioreceptor–analyte interaction, which influences the rate of the power-generating reaction. This can be either enzymatic biofuel cells (EBFCs), which can generate electrical power through highly specific biochemical reactions catalyzed by enzymes immobilized on electrode surfaces or microbial fuel cells (MFCs), which utilize the metabolic activity of electrogenic microorganisms to convert the chemical energy stored in organic matter directly into electricity. These EBFCs show high specificity originating from the enzymatic reactions, making them attractive for detecting particular biomarkers or metabolites.<sup>10</sup> In MFCs, changes in the MFC's power output can correlate with fluctuations in the concentration of the microbial substrate (*e.g.*, measuring biochemical oxygen demand in wastewater) or the presence of substances that inhibit or stimulate microbial activity (*e.g.*, toxins).<sup>11</sup>

For sensors leveraging mechanical (piezoelectric or triboelectric) or thermal energy, the operating principle involves the analyte typically controlling a physical energy conversion process indirectly. In contrast, photoelectrochemical (PEC) systems utilize semiconductor materials (photoelectrodes) that absorb light to generate electron–hole pairs; these charge carriers then drive electrochemical reactions, leading to electricity generation.<sup>12</sup> The produced photocurrent or photovoltage will be highly sensitive to the intensity of incident light.

Interactions between the target analyte and the photoelectrode surface can alter PEC reactions, and this can be used for light-controlled sensing or detection based on analyte-induced changes in the photo-response. Bio-photoelectrochemical cells (BPECs) are specialized systems consisting of both bioelectrocatalytic and photoelectrocatalytic components for converting light and chemical energy into electricity simultaneously.<sup>13</sup> In addition, BPECs hold the advantages of biocompatibility of EBFCs and robustness of PECs.<sup>14</sup>

In both BFC- and PEC-based SPECs, the analyte interaction is linked to the core energy generation mechanism, and the sensing information can be extracted by monitoring the output power of the devices with relatively simple instrumentation. Hence, the processes at the transducer stage can be designed to integrate both the power production and sensing elements closely together to simplify the manufacturing process. Fig. 1 shows the illustration of enzymatic biofuel cells (EBFCs), microbial fuel cells (MFCs) and bio-photoelectrochemical fuel cells (BPFCs).

For the successful realization of BFC- and PEC-based SPECs, it is essential to consider the use of advanced materials with the capability for rapid electron transfer towards the sensor signal readout. In addition, these advanced materials can support both energy conversion and sensing processes through analyte recognition/interaction mechanisms. Various traditional materials like noble metals,<sup>15</sup> carbon nanotubes,<sup>16</sup> graphene,<sup>17</sup> and conducting polymers<sup>18</sup> have been explored for achieving optimal synergy between power generation and sensing performance. However, the stability and biocompatibility of these materials remain significant challenges, which introduce the necessity for novel materials with unique attributes.<sup>19</sup>

Among the emerging candidates, MXenes, a new family of two-dimensional (2D) transition metal carbides, nitrides, and carbonitrides with unique properties, have garnered substantial interest for electrochemical applications including self-powered sensing applications.<sup>20</sup> MXenes are synthesized from their precursor MAX phases *via* selective etching with hydrofluoric acid or alternative etchants. MXenes possess a characteristic combination of unique properties that make them exceptional candidates for developing integrated sensing and power generation platforms.<sup>21</sup> MXenes are represented by the general formula  $M_{n+1}X_nT_x$  (where M is an early transition metal like Ti, V, Mo, *etc.*; X is C or N;  $n = 1-4$ ; and  $T_x$  denotes surface functional groups like  $-F$ ,  $-O$ , and  $-OH$ ).<sup>22</sup> They also exhibit excellent metallic conductivity, which ensures efficient charge transport comparable to or exceeding other traditional electrode materials for electrochemical applications in terms of minimizing internal resistance and maximizing power output.<sup>23</sup> Also, the field of MXenes has been moving towards employing more environmentally friendly chemicals and methods for their synthesis. The application of diluted fluoride-based etchants,<sup>24</sup> electrochemical etching,<sup>25</sup> vapour deposition-based synthetic techniques,<sup>26</sup> and use of waste streams as precursors will help towards making the MXene a sustainable option.<sup>27</sup>

Additionally, the surface functionalization of MXenes renders them hydrophilic and provides numerous anchor



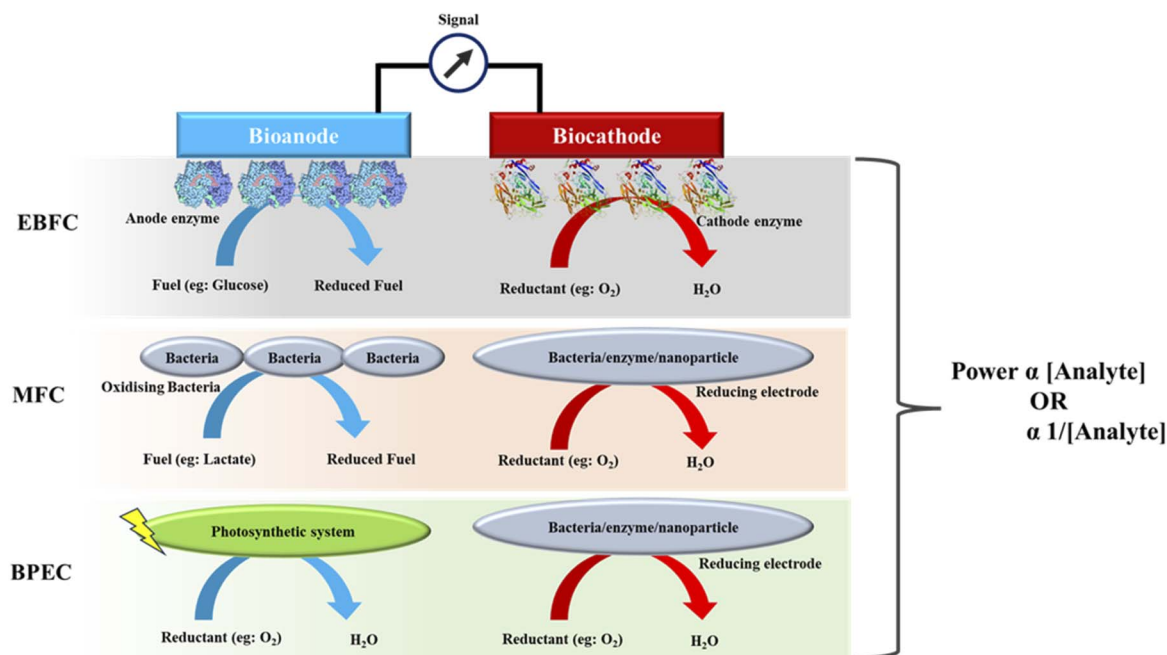


Fig. 1 Illustration of enzymatic biofuel cells (EBFCs), microbial fuel cells (MFCs) and bio-photoelectrochemical fuel cells (BPECs). These systems utilize biological components (enzymes and microbes) and photosynthetic systems to catalyze redox reactions at the anode/bioanode and cathode/biocathode, generating an electrical signal (power), which is typically proportional or inversely proportional to the concentration of a target analyte. The authors have drawn this image.

points for immobilizing enzymes, aptamers, antibodies, or other biorecognition elements, which are essential for highly selective sensing in BFCs.<sup>28</sup> Furthermore, the high specific surface area possessed by these materials enables high catalyst loading, thus enhancing the interaction with the surrounding medium (*e.g.*, electrolyte or biological fluid). Some MXenes also exhibit intrinsic electrocatalytic or co-catalytic activity that can be used to replace other expensive catalysts or enhance efficiency in photoelectrochemical systems.<sup>29</sup> The tunable surface chemistry along with the possibility of diverse elemental compositions and their ability to form advanced hybrid nanocomposites with other materials open new avenues for modifying their electrocatalytic activity towards specific reactions for energy generation involved in BFCs (like oxygen reduction or fuel oxidation) or PECs.<sup>30</sup> The tunable surface chemistry and the presence of hydrophilic groups on MXenes also make these materials friendly for large scale manufacturing because these materials have the ability to be formulated into inks. Formulations of MXenes with biomaterials like enzymes, microbes, and photosynthetic organelles offer attractive opportunities for manufacturing of SPECS.<sup>31,32</sup>

Xu *et al.* employed density functional theory (DFT) to unravel the interfacial electronic structure and energetics of MXene/transition-metal oxide (TMO) heterostructures, using  $-\text{OH}$ ,  $-\text{O}-$ ,  $-\text{F}$ , and mixed-terminated  $\text{Ti}_{n+1}\text{C}_n\text{T}_x$  MXenes coupled with anatase  $\text{TiO}_2$ .<sup>33</sup> Their results reveal that the magnitude of interfacial charge transfer is highly dependent on MXene surface chemistry. Among the various terminations,  $\text{OH}$ -functionalized MXenes exhibited the largest work-function disparity ( $\sim 1.6$  eV for MXene *versus* 6.4 eV for  $\text{TiO}_2$ ), driving

substantial electron migration ( $\sim 0.9$  e  $\text{nm}^{-2}$ ) from the MXene layer into the  $\text{TiO}_2$  interface. This strong charge redistribution not only lowers the interfacial electronic barrier but also enhances adhesion through hydrogen bonding, thereby establishing an electronically coupled and structurally robust junction. Conversely,  $\text{O}$ - or  $\text{F}$ -terminated MXenes exhibited minimal charge transfer and weaker interfacial binding, underscoring the critical role of surface terminations in governing interfacial electronic communication.

While MXene-TMO heterostructures primarily leverage interfacial electron transfer through strong work-function disparities and surface chemistry-driven adhesion, MXene/N-doped graphene hybrids offer a complementary pathway to enhance interfacial kinetics by integrating a highly conductive 2D carbon framework. MXene/N-doped graphene heterostructures exhibit remarkable electrocatalytic efficiency arising from their strong interfacial coupling and accelerated charge-transfer pathways. The DFT calculations also reveal that metallic conductivity of MXenes, combined with the defect-rich, heteroatom-doped graphene network, establishes a seamless electronic interface that minimizes contact resistance and enhances interfacial electron mobility. Nitrogen dopants in graphene introduce localized electronic states near the Fermi level, which act as additional charge reservoirs and facilitate efficient electron tunneling across the heterojunction. Charge density difference maps further confirm pronounced interfacial electron redistribution, indicating strong electronic coupling between MXene and N-doped graphene. This interfacial polarization not only aligns the energy levels between the two components but also optimizes the adsorption energetics of





electroactive species, thereby reducing the kinetic barriers for redox reactions. Collectively, the DFT-derived insights highlight how the synergistic interplay of electronic coupling, defect engineering, and interfacial charge polarization in MXene/N-doped graphene heterostructures provides a robust platform for fast electron-transfer kinetics and stable performance in self-powered electrochemical sensors.<sup>34</sup>

In addition, MXene-polymer interfaces provide another promising strategy to improve the charge-transfer efficiency and interfacial kinetics in SPECSs. As reported using DFT calculations,  $\text{Ti}_3\text{C}_2\text{T}_x$  MXene coupled with polyaniline (PANI) demonstrate pronounced interfacial charge redistribution, with electrons transferring from PANI to MXene due to a favorable Fermi-level alignment. This electron transfer generates an intrinsic interfacial electric field, which facilitates the directional charge flow and significantly reduces the charge-transfer resistance. Partial density of states (PDOS) analysis further reveals the formation of hybridized electronic states at the interface, which act as efficient charge-transport channels. Additionally, this interfacial coupling enhances the adsorption energetics of electroactive species, thereby accelerating redox kinetics crucial for self-powered signal transduction. Looking forward, the rational design of MXene-polymer interfaces, guided by DFT-driven insights, will be critical to overcoming persistent challenges such as interfacial instability, energy loss, and limited operational lifetime, thereby enabling the next generation of highly efficient, durable, and autonomous SPECS platforms.<sup>35</sup>

These inherent advantages of MXenes, which can overcome the limitations of conventional materials in terms of sensitivity, stability, and miniaturization can be utilized in developing powerful building blocks for next-generation, high-performance SPECSs. Indeed, many conventional materials struggle with insufficient signal response to low analyte concentrations (sensitivity), tend to degrade or lose accuracy over extended use or under harsh conditions (stability), and present considerable fabrication challenges for creating compact, portable devices (miniaturization). The following sections in the review explore how these unique properties of MXenes are utilized in the design and fabrication of MXene-based SPECSs. To provide a clear understanding, the review will specifically discuss systems where MXenes serve as active components, including a detailed comparison of key performance characteristics—such as sensitivity, stability, and operational range—when integrated into EBFC-based, MFC-based, and BPEC-based sensors.

## 2. MXenes in enzymatic biofuel cell (EBFC)-based self-powered sensors

The use of enzymes in EBFCs entails some drawbacks like the stability of enzymes and issues with proper immobilization, resulting in lesser power production. To overcome these limitations, Ji *et al.* introduced an innovative biofuel cell-based self-powered sensor design for the detection of lead ions.<sup>36</sup> They utilized two-dimensional lamellar gold nanoparticles- $\text{Ti}_3\text{C}_2\text{T}_x$

(AuNPs- $\text{Ti}_3\text{C}_2\text{T}_x$ ) heterostructures for the anode, in which the AuNPs provided glucose oxidase-like catalytic activity, and this can be used to replace the potentially unstable enzymes. In addition, the  $\text{Ti}_3\text{C}_2\text{T}_x$  MXene provides signal amplification owing to their excellent charge storage capacity, which can solve the potential issues of low current production. In the sensor design, they used doped carbon-based nanosheets as the cathode with promising oxygen reduction reaction catalytic activity. Together with these anode and cathode modifications, the developed enzyme-free biofuel cell was able to detect lead ions in the range of 0.01–7500 nM with a limit of detection (LOD) of 0.43 pM along with realization of practical applications using human plasma samples.

Even though SPECSs show great potential, they are often limited in practical applications due to low energy conversion efficiency and limited selectivity, especially in complex samples. As an approach to mitigate these limitations, Sun *et al.* reported a novel self-powered biosensor employing EBFCs, specifically for ultrasensitive CD44 detection.<sup>37</sup> CD44 is a cell-surface molecule involved in many cellular processes and acts as a key biomarker and therapeutic target, especially in cancer metastasis. Hence, the sensitive and specific detection of CD44 is highly essential for diagnostic applications which require advanced sensor platforms. They have synthesized an MXene-AuNP composite, as shown in Fig. 2(a). The developed biosensor consisted of a Au-MXene modified bioanode conjugated with

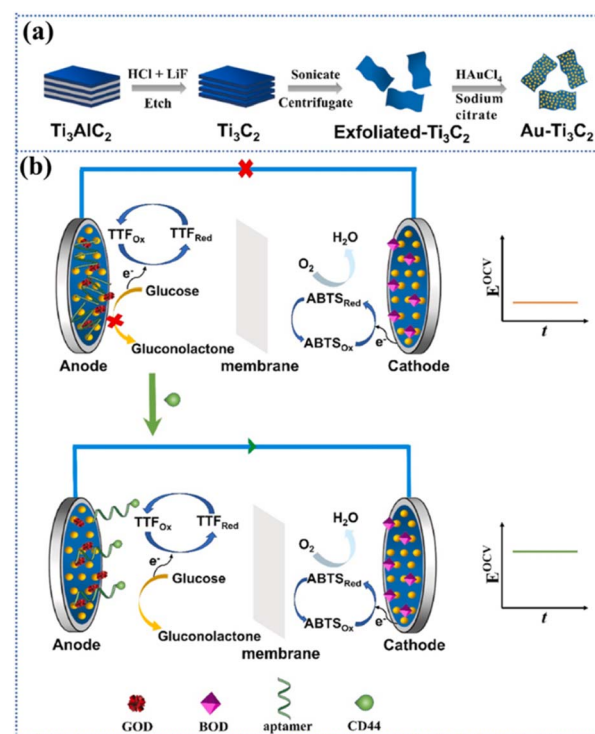


Fig. 2 (a) Schematics showing the synthesis of a Au-MXene composite; (b) the schematic illustration of fabrication of the EBFC self-powered sensor with a bioanode and a biocathode and changes in the OCV upon binding with the CD44 protein and the immobilized aptamer. Reproduced with permission from ref. 37, copyright© 2024 Elsevier B.V.



glucose oxidase (GOD) and an aptamer and a bilirubin oxidase (BOx) conjugated Au–MXene modified biocathode, as shown in Fig. 2(b). Initially, the aptamer with high insulation on the bioanode hindered the electron transfer and produced a low open circuit voltage (OCV). When the target CD44 protein was captured by the aptamer at the bioanode, it produced structural changes at the electrode surface, which led to the transfer of electrons and increased the OCV in proportion to the analyte concentration. This clever sensor design achieved a promising LOD of  $0.052 \text{ ng mL}^{-1}$ , excellent selectivity and stability, proving effective for sensing in real blood samples without any special pre-treatment and highlighting its potential for early cancer diagnosis.

Ji *et al.* developed a novel enzyme-free intra-capacitive bi-fuel cell (ICBFC)-based self-powered sensor for the electrochemical detection of endocrine-disrupting phthalates like di(2-ethylhexyl)phthalate (DEHP).<sup>38</sup> The sensor design included the integration of a ternary heterostructure capacitive anode and a sensing-interface cathode within a single chamber. The anode was made of  $\text{Ti}_3\text{C}_2\text{T}_x$  MXene, ultra-small AuNPs, and polypyrrole (PPy) NPs in which AuNPs enabled efficient enzyme-free glucose oxidation, while the synergistic combination of MXene's double-layer capacitance and pseudocapacitance of PPy enhanced the charge storage. This sophisticated ICBFC-based self-powered sensor demonstrated a promising LOD of  $9.51 \text{ pg L}^{-1}$  for DEHP over a wide linear range, highlighting its potential for rapid, on-site environmental monitoring and public health protection.

In another recent work, Xiao *et al.* reported a flexible, self-powered biosensor for lactate detection based on carbon cloth electrodes immobilized with lactate oxidase (LOx) and BOx on reduced graphene oxide (rGO).<sup>39</sup> Here, MXene was incorporated into a polypyrrole/polyurethane hydrogel and used as a substrate for sensor assembly for placing the electrodes. This integration of MXene hydrogel enhanced the current output by 15-fold due to improved electron mobility and ionic conductivity of MXenes. The developed sensor produced a maximum power density of  $\sim 3 \mu\text{W cm}^{-2}$  at 100 mM lactate and showed a linear current response in the physiological window of lactate. This can be used as a biocompatible and scalable route for future wearable applications, enabling accurate, continuous, and self-powered sensing of lactate in physiological environments.

### 3. MXenes in biophotoelectrochemical (BPEC)-based self-powered electrochemical sensors

Self-powered photocatalytic fuel cell-based sensors integrating bioelement recognition with fuel concentration-dependent output power can be used for electrochemical analysis. The problems with existing self-powered photocatalytic fuel cell-based sensors are poor energy conversion efficiency and unsuitability for routine use. To address these problems, Qiu *et al.* designed a multi-functional self-powered photocatalytic

fuel cell platform for the detection of ochratoxin A, which is a toxic and potentially carcinogenic mycotoxin produced by certain molds.<sup>40</sup> Here, the photoanode of the sensor was constructed with a  $\text{Ti}_3\text{C}_2\text{T}_x$  MXene– $\text{TiO}_2$  composite, and the cathode was modified with Prussian blue (PB), enabling a visual checking capability through color change along with electrical signals. For realizing the sensing mechanism, mesoporous silica nanoparticles (MSNs) were used as nanocontainers loaded with glucose and aptamers specific to ochratoxin A. The schematics of the sensor fabrication and how the bioresponsive controllable glucose release helps in the detection of ochratoxin A are given in Fig. 3. When the analyte reacts with the aptamer, the glucose is released from mesoporous silica nanoparticles, which powers the photocatalytic fuel cell. The released glucose is photo-oxidized by the  $\text{Ti}_3\text{C}_2\text{T}_x$  MXene– $\text{TiO}_2$  composite under visible light illumination, and the produced electron can reduce PB, which results in a high output power of  $23.516 \mu\text{W cm}^{-2}$ ; the developed sensor showed promising analytical performance towards ochratoxin A in the range of 0.2–20 ppb with an LOD of 0.0587 ppb.

In another work, Jin *et al.* reported a novel self-powered biosensor by uniquely integrating a photocatalytic fuel cell with a molecular imprinting polymer (MIP) for the detection of aflatoxin B1, which is a highly potent carcinogenic mycotoxin.<sup>41</sup> Here, the issue of energy conversion efficiency is tackled by using a  $\text{MoS}_2$ – $\text{Ti}_3\text{C}_2\text{T}_x$  MXene heterojunction on indium tin oxide (ITO) as a photoanode within the photocatalytic fuel cell which can harness light energy more effectively. The cathode was made by a combination of hemin and graphene to catalyze the reduction of hydrogen peroxide, as shown in Fig. 4. Simultaneously, the selectivity issue is directly addressed by incorporating the MIP, which is designed to specifically capture the target analyte aflatoxin B1 ( $\text{AFB}_1$ ) even in the presence of interfering agents. In the absence of  $\text{AFB}_1$ , the photogenerated holes of photoanodes could promote the oxidation of ascorbic acid (AA) and produces an OCV. When  $\text{AFB}_1$  binds to the cavities of MIP, it affects the OCV of the system, and this change can be used for the specific and sensitive detection of  $\text{AFB}_1$  with an LOD of  $0.73 \text{ pg mL}^{-1}$ , as illustrated in Fig. 4. The developed

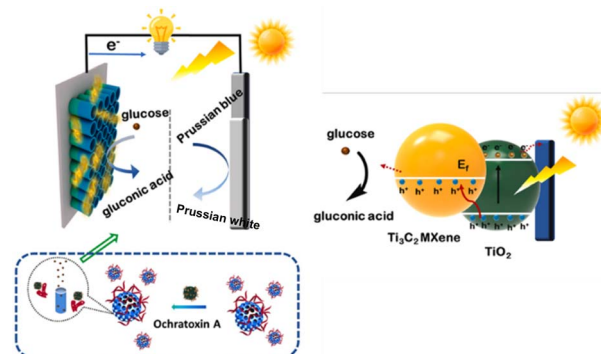


Fig. 3 Schematic illustration of the mechanism of self-powered photocatalytic fuel cell (PFC)-based sensors using a  $\text{Ti}_3\text{C}_2\text{T}_x$  MXene– $\text{TiO}_2$  composite as the photoanode and Prussian blue (PB) as the cathode for the detection of ochratoxin A. Reprinted with permission from ref. 40. Copyright© 2023, published by Elsevier B.V.



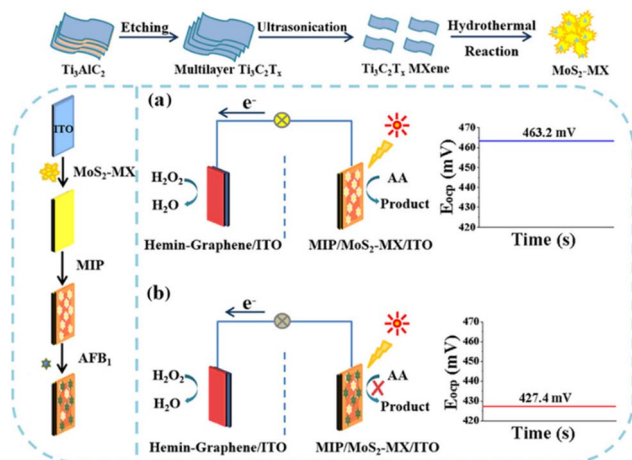


Fig. 4 Schematics showing the self-powered photocatalytic fuel cell-based biosensor for AFB<sub>1</sub> detection. The synthesis of the MoS<sub>2</sub>-Ti<sub>3</sub>C<sub>2</sub>T<sub>x</sub> MXene heterojunction and the fabrication of photoanode are given. (a) The conversion of AA into products in the absence of AFB<sub>1</sub> produces an OCV and (b) the OCV reduces in the presence of AFB<sub>1</sub> as the conversion of AA is blocked. Reprinted with permission from ref. 41. Copyright© 2021, American Chemical Society.

sensor uses this dual approach of MIP for specific target recognition and MXene for efficient light-driven signal conversion for the photocatalytic fuel cell.

Ultrasensitive detection of potent toxins like microcystin-RR (MC-RR) is highly critical for environmental safety evaluation

and need to fabricate advanced portable and real time sensors with efficient signal amplification for sensitive detection. Towards this aspect, Sun *et al.* constructed a photo-driven self-powered BPEC aptasensor for MC-RR using the Ti<sub>3</sub>C<sub>2</sub>T<sub>x</sub>/ZnIn<sub>2</sub>S<sub>4</sub> heterojunction as the photoanode and Cu<sub>2</sub>O as the photocathode.<sup>42</sup> The Ti<sub>3</sub>C<sub>2</sub>T<sub>x</sub> MXene in the system enhances charge separation in addition to providing a large surface area for immobilization of the MC-RR specific aptamer. When MC-RR binds to the aptamer, it causes a 'signal-off' mechanism due to steric hindrance, which reduces the photocurrent. In addition, they integrated a matching capacitor, boosting the sensitivity by 22-fold and proposed a USB-sized micro-workstation for capturing instantaneous signals to make the system portable. Under optimal conditions, this multi-amplification system achieved the photocurrent in a linear relation with the concentration of MC-RR with an extremely low LOD of 0.033 pM and demonstrated the practical applicability of the system in fish samples.

In a different approach, a novel dual-power-peak photofuel cell (PFC)-based self-powered sensor has been developed for the detection of chloramphenicol by introducing dual peak output signals for enhancing the detection accuracy.<sup>43</sup> They have utilized persulfate as an initiator for getting a dual peak response in the PFC system, which can enhance charge separation and generate a second power peak in the output signal. The photoanode was made of fluorine-doped tin oxide (FTO) modified with BiVO<sub>4</sub> and V<sub>2</sub>C MXene, followed by modification with an aptamer, as seen in Fig. 5(a). The incorporation of V<sub>2</sub>C MXene accelerates electron transfer, boosting photoelectric conversion efficiency, while the aptamer provides specific recognition of chloramphenicol. FTO modified with molybdate hexacyanoferrate (MoHCF) was used as a photocathode, as shown in Fig. 5(b). The construction of the dual-power-peak photocatalytic fuel cell-based self-powered sensor is given in Fig. 5(c). When chloramphenicol binds to the aptamer on the photoanode, the output signal of the sensor, including two power peaks, changed linearly with the concentrations of chloramphenicol (Fig. 5(d)). The quantification of chloramphenicol based on these dual power peaks allowed sensitive detection with an LOD of 0.17 pM over a linear range of 0.5 pM to 3 nM, demonstrating a promising strategy for developing highly sensitive and specific multi-signal self-powered sensors.

#### 4. MXenes in other self-powered electrochemical sensors

Recently, zinc-air battery (ZAB)-driven self-powered biosensors have shown great potential for the detection of trace analytes, demonstrating high output potential and excellent stability and sensitivity.<sup>44</sup> Most ZABs can generate high output voltage and energy density and can be used in biosensing applications. The major concern in the fabrication of superior ZAB-assisted PFC biosensors is to develop an efficient photocatalyst with high photocatalytic ability, fast electron transfer and high bioaffinity towards bioprobes.<sup>45</sup> In this context, MXenes are considered as promising candidates in comparison with other 2D materials,

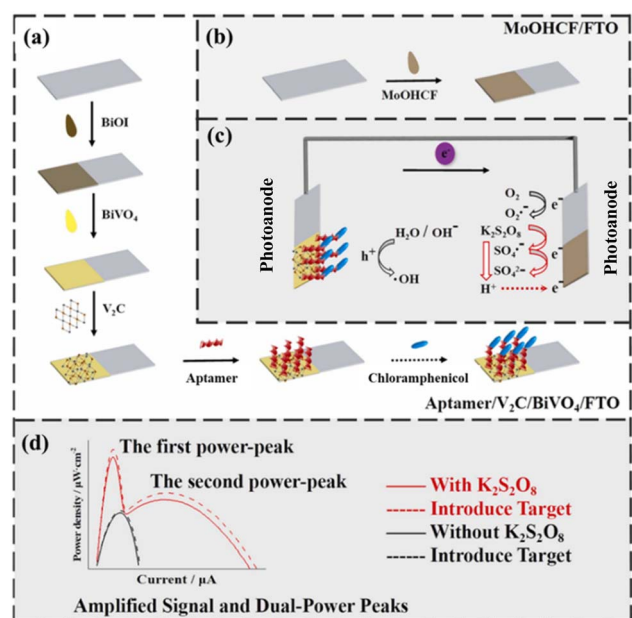


Fig. 5 The schematic showing the fabrication of a dual-power-peak photofuel cell (PFC)-based self-powered sensor for the detection of chloramphenicol. (a) Fabrication of the photoanode. (b) Fabrication of the photocathode. (c) Construction of the dual-power-peak PSPS combining the photoanode and photocathode. (d) Schematic illustration showing the dual-power-peak detection configuration in the presence of K<sub>2</sub>S<sub>2</sub>O<sub>8</sub>. Reprinted with permission from ref. 43. Copyright© 2023, Elsevier B.V. All rights reserved.





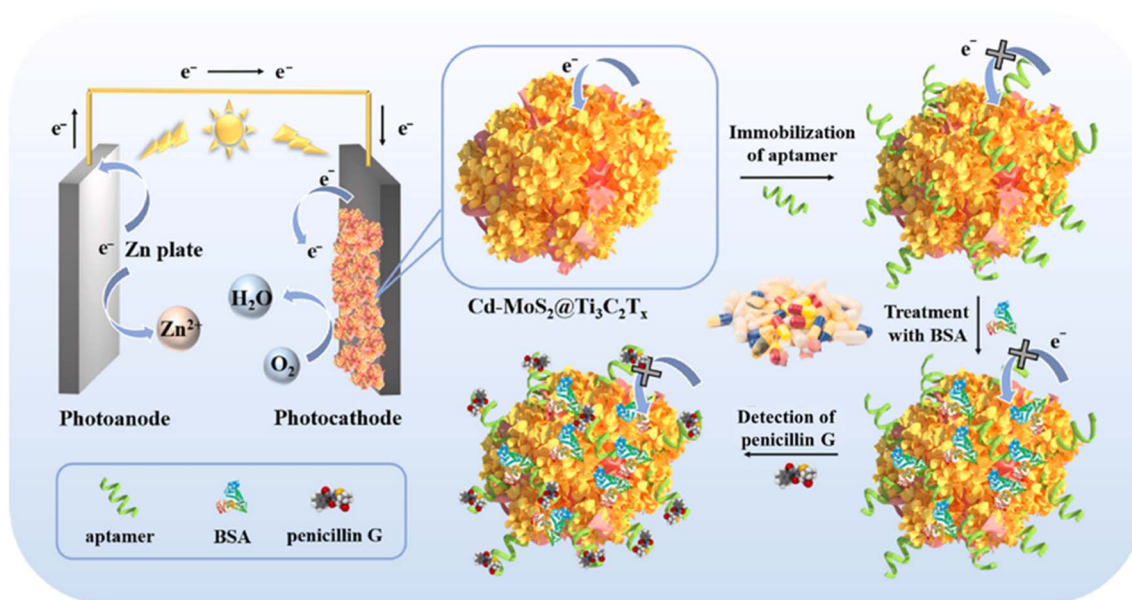


Fig. 6 Schematic diagram showing the fabrication steps for the photo-assisted ZAB-driven self-powered aptasensor for the detection of penicillin G and the mechanism of detection of penicillin G. Reprinted with permission from ref. 47. Copyright© 2023, Elsevier B.V.

considering high electrical conductivity, hydrophilicity and easy surface functionalization.<sup>46</sup>

Various other self-powered sensors have been developed by using MXenes as one of their components. In this aspect, Liu *et al.* developed a novel dual-modal zinc–air battery (ZAB) driven self-powered electrochemical aptasensor based on the heterojunction of V<sub>2</sub>CT<sub>x</sub> MXene and bimetallic CoNi-layered double hydroxide (CoNi-MLDH) for the detection of cortisol.<sup>46</sup> They utilized V<sub>2</sub>CT<sub>x</sub> nanosheets as scaffolds for the *in situ* growth and subsequent formation of CoNi-MLDH nanosheets. The V<sub>2</sub>CT<sub>x</sub> MXene in the CoNi-MLDH composite enhances the electrochemical activity, while the CoNi-LDH enhances the surface area, functionality, oxygen reduction activity, and aptamer affinity of the composite. By utilizing these advantages, the developed ZAB driven self-powered aptasensor was able to achieve a very low LOD of 0.17 fg mL<sup>-1</sup> for cortisol.

In another work, a similar ZAB-based self-powered aptasensor was proposed by Liu *et al.* for the detection of penicillin G by using a Zn plate photoanode and a heterojunction made of cadmium-doped MoS<sub>2</sub> nanosheets grown on Ti<sub>3</sub>C<sub>2</sub>T<sub>x</sub> MXene (Cd–MoS<sub>2</sub>@Ti<sub>3</sub>C<sub>2</sub>T<sub>x</sub>) as the photocathode.<sup>47</sup> Fig. 6 shows the schematics of the fabrication of a photo-assisted ZAB-driven self-powered aptasensor and detection process by binding the aptamer with penicillin G. The enhanced light absorption, high photoelectric conversion efficiency, and more catalytic active sites of this heterojunction boost the ZAB output voltage to 1.43 V under UV-vis light irradiation. The resulting self-powered aptasensor displayed an ultralow LOD of 0.06 fg mL<sup>-1</sup> for penicillin G, with promising specificity and stability, offering a promising portable sensor for the detection of antibiotics.

## 5. Critical bottlenecks in self-powered electrochemical sensors (SPECSSs): views from MXene and broader platforms

Self-powered electrochemical sensors encounter notable energy-related limitations due to the characteristics of their energy harvesters, namely triboelectric nanogenerators. These devices are adept at generating high voltages, but their output currents are often quite modest. This disparity can restrict sensor effectiveness, especially for applications that need robust electrochemical activity or fast responses. Attempts to boost energy output through microstructuring surfaces provide some improvements, but they also introduce challenges related to material degradation and loss of performance stability over time. Issues like fatigue or detachment at electrodes and interfaces can further undermine the reliability of the sensor, underscoring the necessity for wear-resistant materials and stable surface engineering.

The path to functional integration of energy harvesters with sensing circuits is also complicated by the variable and pulsed nature of the generated electrical signals. These fluctuations can make accurate signal measurement difficult and may lead to unwanted phenomena at the electrode, such as the build-up of polarization or secondary chemical reactions that are not part of the intended sensing process. When several energy harvesting elements are combined, phase mismatches can occur, leading to irregular signal shapes and increased risk of sensor aging due to surface passivation. While using alternative current generation regimes can sometimes help mitigate these effects, it adds to the complexity of sensor design and the need







Table 1 Comparative analysis of self-powered electrochemical sensors (SPECSS): MXenes vs. other nanomaterials

Anode	Cathode	Analyte	LOD	Dynamic range	Construction and performance metrics ( $P_{\text{max}}/E_{\text{OCV}}$ ) at the baseline	Stability	Ref.
Two-dimensional lamellar gold nanoparticles- $\text{Ti}_3\text{C}_2\text{T}_x$ ( $\text{AuNPs-Ti}_3\text{C}_2\text{T}_x$ ) heterostructures	Doped carbon-based nanosheets	Lead ion ( $\text{Pb}^{2+}$ )	0.43 pM	0.01–7500 nM	Beaker-based $E_{\text{OCV}}$ : 367 mV	~92% of the initial level after 45 days	36
MXene-AuNP composite modified with glucose oxidase (GOx) and an aptamer $\text{Ti}_3\text{C}_2\text{T}_x$ MXene, ultra-small AuNPs, and polypyrrole (PPy) NPs (ternary heterostructure capacitive anode)	Au-MXene modified with bilirubin oxidase (BOx)	CD44 protein	0.052 ng $\text{mL}^{-1}$	0.5–1000 ng $\text{mL}^{-1}$	Beaker-based $P_{\text{max}}$ : ~1 $\mu\text{W cm}^{-2}$ $E_{\text{OCV}}$ : 390 mV	~97% after 15 days	37
$\text{Ti}_3\text{C}_2\text{T}_x$ MXene- $\text{TiO}_2$ composite photoanode	A sensing-interface cathode within a single chamber	$\text{Di(2-ethylhexyl)phthalate (DEHP)}$	9.51 pg $\text{L}^{-1}$	0.05 to 100 000 ng $\text{L}^{-1}$	Beaker-based Anode is non-enzymatic glucose-based, which drives the cathode-based DEHP sensor	93.2% after 30 days	38
$\text{MoS}_2\text{-Ti}_3\text{C}_2\text{T}_x$ MXene heterojunction on indium tin oxide (ITO)	Prussian blue (PB) cathode	Ochratoxin A	0.0587 ppb	0.2–20 ppb	Beaker-based $P_{\text{max}}$ : ~15.015 $\mu\text{W cm}^{-2}$ $E_{\text{OCV}}$ : ~440 mV	85.2% of the initial level after 7 days	40
$\text{Ti}_3\text{C}_2\text{T}_x/\text{ZnIn}_2\text{S}_4$ heterojunction photoanode	Hemin and graphene composite	Aflatoxin B1 (AFB1)	0.73 pg $\text{mL}^{-1}$	0.01–1000 ng $\text{mL}^{-1}$	Beaker-based $E_{\text{OCV}}$ : ~465 mV in PBS, milk, oil, and maize	97% of the initial level after 7 days	41
$\text{BiVO}_4$ and $\text{V}_2\text{C}$ MXene on fluorine-doped tin oxide (FTO)	$\text{Cu}_2\text{O}$ photocathode	Microcystin-RR (MC-RR)	0.033 pM	0.1 to 100 pM	Portable device $P_{\text{max}}$ : ~26 $\mu\text{W}$ $E_{\text{OCV}}$ : ~450 mV	Unchanged after continuous cycling every 7 days	42
$\text{V}_2\text{CT}_x$ MXene and bimetallic CoNi-layered double hydroxide (CoNi-MLDH) heterojunction	Molybdate hexacyanoferrate (MoHCF)	Chloramphenicol	0.17 pM	0.5 pM to 3 nM	Beaker-based $P_{\text{max}}$ : 0.626 $\mu\text{W cm}^{-2}$ under light irradiation	97.99% signal after 6 cycles every 2 days	43
Zinc (Zn) plate photoanode	Zinc (Zn) plate anode	Cortisol	0.17 fg $\text{mL}^{-1}$	10 fg $\text{mL}^{-1}$ to 100 ng $\text{mL}^{-1}$	Device based on a glass substrate $E_{\text{OCV}}$ : 1130 mV	98.49% after 15 days	46
Cadmium-doped $\text{MoS}_2$ on the $\text{Ti}_3\text{C}_2\text{T}_x$ MXene ( $\text{Cd-MoS}_2@\text{Ti}_3\text{C}_2\text{T}_x$ ) heterojunction photocathode	Cadmium-doped $\text{MoS}_2$ on the $\text{Ti}_3\text{C}_2\text{T}_x$ MXene ( $\text{Cd-MoS}_2@\text{Ti}_3\text{C}_2\text{T}_x$ ) heterojunction photocathode	Penicillin G	0.06 fg $\text{mL}^{-1}$	1.0 fg $\text{mL}^{-1}$ to 0.1 ng $\text{mL}^{-1}$	Beaker-based $P_{\text{max}}$ : ~2500 $\mu\text{W cm}^{-2}$ $E_{\text{OCV}}$ : ~1100 mV	96.4% after 20 days	47
Pencil graphite-MWCNT/pyrroloquinoline quinone-dependent glucose dehydrogenase (PQQGDH)	Pencil graphite-MWCNT/bilirubin oxidase (BOx)	Glucose	0.084 mM	Up to 1 mM	Beaker-based $P_{\text{max}}$ : ~2.5 $\mu\text{W cm}^{-2}$ $E_{\text{OCV}}$ : ~450 mV	94% after 12 days	56
Carbon paper (CP)/ultrathin hollow carbon	DNA1/UHCS/AuNPs/CP	L-Cysteine	2.2 nM	0.01–5 $\mu\text{M}$	Beaker-based $E_{\text{OCV}}$ : ~360 mV	97% after 2000 s	57



Table 1 (Contd.)

Anode	Cathode	Analyte	LOD	Dynamic range	Construction and performance metrics ( $P_{\max}/E_{\text{OCV}}$ ) at the baseline	Stability	Ref.
shells (UHCS)/gold nanoparticles (AuNPs)/polydopamine film/laccase							
Carbon cloth/AuNPs/graphdiyne/glucose oxidase/bovine serum albumin	Carbon cloth/AuNPs/graphdiyne/AuNPs/T-DNA/MCH/DNA nanorods	miRNA-141	21.9 aM	0.0001 to 100 pM	Beaker-based $E_{\text{OCV}}$ : ~175 mV	96.0–97.3% after 12 days	58
Crystalline polymeric carbon nitride/SWCNT film	SWCNT/Pt NPs	Peroxide	0.006 mM	0–1.0 mM	Microfluidic-based Photoelectrochemical sensing mechanism regulated by electrocatalytic current	Unchanged for 7 days	59

for precise electrical matching. These SPECSs inherently face the challenge of limited energy conversion efficiency due to constrained power harvesting, inefficient interfacial coupling, and low signal transduction rates.<sup>48</sup>

Another central challenge lies in the properties and robustness of the electrode materials themselves. While MXene electrodes offer high electrical conductivity and rich surface terminations, practical issues such as restacking of nanosheets and agglomeration significantly reduce the accessible surface area and block redox-active sites, resulting in lower energy output and diminished sensor sensitivity. Even beyond MXenes, non-MXene materials like carbon nanotubes and metal oxides also hit similar efficiency barriers, such as poor wettability, sluggish electron-ion transport, and weak electrode-solution coupling, hampering comprehensive energy-to-signal conversion in autonomous sensing configurations.<sup>49</sup>

In addition to efficiency, operational instability poses a critical limitation to SPECS lifespan, particularly in wearable or biological environments. MXene materials are prone to oxidation, especially under exposure to humidity or oxidative conditions, leading to conductivity degradation and signal drift over time. Biological deployment further introduces biofouling, molecular adsorption, and environmental interference, all of which can obstruct electrode surfaces and disrupt consistent sensing performance. Similarly, non-MXene systems such as conductive polymers or metal oxide sensors face structural deformation, polymer degradation, or loss of receptor function limitations that shorten device lifetimes and affect repeatability.<sup>50</sup>

Finally, scalability, reproducibility, and sensor specificity remain formidable obstacles to commercialization. MXene fabrication often depends on harsh etching techniques, leading to variability in surface termination (–O, –OH, and –F), flake size, and defect density—factors that directly affect electrochemical performance and batch-to-batch consistency. On the non-MXene side, heterogeneous hybrids of organic and inorganic elements often struggle with inconsistent receptor attachment, limited analyte specificity, and low selectivity, reducing the accuracy in real-world deployments. Addressing these challenges will require green, standardized manufacturing processes, robust surface chemistries, and integrated receptor design to ensure a reproducible, selective, and commercially viable SPECS platform.<sup>48,51</sup>

In sum, advancing self-powered electrochemical sensors to practical, widespread use will demand solutions that improve both energy harvesting and material stability while also enabling reliable mass production. Progress toward more sustainable production, better integrated circuit management, and the development of robust, durable interfaces will be key steps. Only by tackling these challenges in concert will the promise of self-powered sensing technologies be fully realized.

A solid foundation for the advancement of SPECS has been laid by several key research efforts. Wang and coworkers were pioneers in the field, establishing the concept of wearable self-powered sensors and on-body power grids.<sup>52,53</sup> This work created a crucial framework for integrating energy harvesting with sensing technology. Building on this, Yin *et al.* demonstrated the use of passive perspiration-based biofuel cells,

a concept that can be realized with great efficiency using MXenes due to their high conductivity, hydrophilicity, and ability to preserve the function of power-generating biocomponents.<sup>54</sup> This work provides a clear roadmap for harnessing the unique properties of MXenes in practical applications. Furthermore, a critical question regarding the biocompatibility of MXenes for wearable applications was addressed by Gao and coworkers, who successfully developed an MXene-based platform for monitoring female hormones, thereby proving its viability for direct human use.<sup>55</sup>

Based on the provided data, a direct quantitative comparison between MXene-based SPECSs and conventional materials is challenging due to the early stage of MXene research and diverse device architectures. However, qualitative contrasts can be made in this aspect. MXene-based devices often demonstrate comparable or superior sensitivity and fast response times for specific analytes, as shown by the pM-level detection limits for lead ions and the dynamic ranges for other proteins. For instance, the Au-MXene device for CD44 protein shows versatility with its wide dynamic range. Additionally, MXenes show promising stability with a 98.49% signal retention after 15 days for a cortisol sensor.<sup>37</sup> This is a significant finding as stability is often a major challenge for nanomaterial-based devices (Table 1). Table 1 shows a comparative analysis of SPECSs based on MXenes with other nanomaterials. An analysis of Table 1 indicates that MXene- and non-MXene-based SPECSs exhibit similar stability and performance metrics. In addition, MXene-based modifications are expected to possess better aqueous solution processibility than their pristine carbon counterparts, which makes them more environmentally sustainable for use in SPECSs. However, the heterogeneity in reported electrode construction—specifically the varying methodologies, protocols, and modification layers—precludes a comparison of the true stability performance across these reports. A proposed benchmark for MXene-based SPECSs is the attainment of higher stability metrics using smaller form factors.

The current lab-scale, beaker-based nature of these devices suggests a low Technology Readiness Level (TRL), likely TRL 1 to TRL 4. This means the primary focus is on establishing fundamental principles and feasibility in a controlled environment. Real-world performance under various environmental conditions like humidity and temperature is typically assessed at higher TRLs (*e.g.*, TRL 5 and 6). Therefore, further research is necessary to move these technologies from the lab to a fabricated device that can be systematically tested under real-world conditions to address these concern and evaluate its resilience to environmental stressors.

## 6. Stability of MXenes

The chemical and environmental vulnerability of MXenes when exposed to air or water significantly restricts their deployment in practical systems. Surface groups such as hydroxyl, oxygen and fluorine form reactive sites that initiate oxidation. Researchers therefore pursue two main approaches. One aims to improve the intrinsic resilience of MXene by refining synthesis and reducing defect density. The other focuses on

postsynthesis stabilization through controlled storage conditions, antioxidant additives or protective coatings.

### 6.1. Thermodynamic stability of MXenes

MXenes exhibit significant thermodynamic instability due to their high surface energy, which makes them prone to degradation even under mild conditions. Surface terminations, such as  $-\text{OH}$ ,  $-\text{O}$ , or  $-\text{F}$ , commonly present in MXenes, further aggravate this issue by increasing their reactivity with environmental agents. For example,  $\text{Ti}_3\text{C}_2\text{T}_x$  MXenes are particularly prone to oxidation under ambient conditions, leading to the formation of  $\text{TiO}_2$  and a loss of electrical conductivity. Studies have shown that even brief exposure to air can result in measurable degradation, with oxidation rates heavily influenced by the density and type of surface terminations. Elevated temperatures accelerate these transformations, with thermal decomposition often leading to the conversion of MXenes into metal oxides completely, and this phenomenon is particularly problematic for high-temperature applications. For instance,  $\text{Ti}_3\text{C}_2\text{T}_x$  MXenes, when subjected to temperatures above 400 °C, decompose into anatase or rutile  $\text{TiO}_2$ , as reported in thermal stability studies.<sup>60</sup>

The degree of hydrophilicity observed in these materials was found to depend heavily on both etching media, whether it is a single acid like HF or a combination of acids such as  $\text{H}_2\text{SO}_4$  and HF or HCl and HF. Interestingly,  $\text{Ti}_3\text{C}_2\text{T}_x$  exhibited a greater retention of structural water when fewer oxygen-based terminations were present on the surface. Furthermore, employing milder etching conditions or mixed acid systems led to improved thermal robustness by minimizing defect sites during synthesis. The thermal durability of MXenes is closely linked to their intrinsic structure and elemental makeup. Among them,  $\text{Ti}_3\text{C}_2\text{T}_x$  exhibits superior heat resistance compared to  $\text{Mo}_2\text{CT}_x$  and  $\text{Nb}_2\text{CT}_x$ , both of which possess fewer atomic layers. Between the latter two,  $\text{Mo}_2\text{CT}_x$  is thermally more robust than  $\text{Nb}_2\text{CT}_x$ .<sup>61</sup>

### 6.2. Key influences on the oxidative stability of MXenes

The stability of MXenes is strongly influenced by their intrinsic chemical composition and microstructural features, particularly the type of metal layers and the surface terminations. Zhang *et al.* examined the oxidation response of  $\text{Nb}_4\text{C}_3\text{T}_x$  MXenes in a  $\text{CO}_2$  atmosphere at 850 °C and reported the development of a multilayered structure decorated with uniformly distributed  $\text{Nb}_2\text{O}_5$  nanoparticles across the nanosheet surface. Their study revealed that  $\text{Nb}_4\text{C}_3\text{T}_x$  is considerably more resistant to oxidation than  $\text{Ti}_3\text{C}_2\text{T}_x$ , which undergoes oxidation at much lower temperatures, around 500 °C, under  $\text{CO}_2$  flow.<sup>62</sup>

Numerous research ideas have highlighted that the structural integrity of MXenes is governed by a combination of external chemical conditions and inherent material properties, such as atmospheric exposure, temperature, compositional variations, microstructural features, and interactions with aqueous environments. Furthermore, even MXenes sharing the same chemical composition can display markedly different oxidation behaviours, primarily due to variations in their synthesis techniques and processing conditions.





Extensive investigations have been carried out to understand the thermal and chemical stability of MXenes under different atmospheric conditions such as vacuum, inert, oxidizing, and reducing environments. For instance,  $\text{Ti}_3\text{C}_2$  MXenes have been reported to remain structurally stable in an argon atmosphere even at elevated temperatures of up to 800 °C. In contrast, when subjected to oxygen-rich conditions, oxidation begins at relatively low temperatures (200 °C), leading to the uniform formation of anatase across the surface. Upon heating to 1000 °C, this anatase phase further transforms completely into rutile.<sup>63,64</sup> A detailed evaluation of  $\text{V}_2\text{CT}_x$  MXenes was carried out by Thakur *et al.*, who examined their stability in air,  $\text{CO}_2$ ,  $\text{H}_2$ , and  $\text{N}_2$  atmospheres at temperatures of up to 600 °C. They reported that above 300 °C,  $\text{V}_2\text{CT}_x$  readily oxidized in air or  $\text{CO}_2$ , producing  $\text{V}_2\text{O}_5$  and other  $\text{VO}_x$  phases, along with a complete collapse of the layered architecture. Under a reducing  $\text{H}_2$  atmosphere, however, partial retention of the layered structure was observed. Exposure to  $\text{N}_2$  led to mild oxidation, attributed to trace  $\text{H}_2\text{O}$  molecules incorporated during the synthesis process, which reacted with the surface groups of  $\text{V}_2\text{CT}_x$ .<sup>65</sup>

The oxidation of MXenes occurs more rapidly when they are dispersed in aqueous media compared to their freestanding form. Earlier studies attributed this instability mainly to dissolved  $\text{O}_2$  in water. However, more recent evidence suggests that MXenes are inherently more reactive toward  $\text{H}_2\text{O}$  molecules than toward dissolved oxygen.<sup>66</sup> Beyond neutral solutions, investigations have been extended to alkaline and oxidizing environments. Doo *et al.* demonstrated that pH plays a critical role in dictating the oxidation pathway of aqueous  $\text{Ti}_3\text{C}_2$  dispersions. They proposed a distinct mechanism in which the terminal  $-\text{OH}$  groups interact with either  $\text{H}^+$  or  $\text{OH}^-$  ions, generating different reaction intermediates depending on the pH.<sup>67</sup> Complementing this, Zhao *et al.* showed that alkaline conditions accelerate MXene oxidation, where hydroxyl ions significantly enhance the conversion of Ti species. This conclusion was supported by X-ray photoelectron spectroscopy (XPS) analysis, which revealed an increased proportion of  $\text{Ti(IV)}$  species in basic media.<sup>68</sup> The stability and performance of MXenes depend on multiple factors, including the method of synthesis, the nature of surface terminations, structural stability, and particle size, all of which need to be carefully optimized to ensure their effective use in a wide range of applications.

### 6.3. Extending the lifetime of MXenes through oxidation mitigation

The limited stability of MXenes in ambient air and aqueous environments remains a key obstacle to their practical utilization. To overcome this challenge, significant research has focused on improving their resistance to degradation or alternatively designing systems that operate under non-aqueous conditions. This need has stimulated intensive efforts to suppress oxidation and structural breakdown, ultimately broadening the technological potential of MXenes. Reported approaches include strict regulation of storage environments and complete isolation from oxygen and moisture. In addition,

the incorporation of antioxidant agents such as polyphosphoric anions and ascorbates has been shown to effectively slow down oxidation processes.

Oxidation in MXenes is often initiated at reactive surface terminations, particularly hydroxyl groups, which are highly vulnerable to oxidative attack. One approach to suppress this process involves the removal of surface terminations through thermal annealing under vacuum or inert environments. Such treatments enhance the inherent thermal stability of MXenes and extend their applicability in high-temperature settings. For instance, Wang *et al.* demonstrated that MXenes stripped of surface terminations could withstand heating up to 1200 °C under an argon atmosphere.<sup>69</sup> Similarly, Zhao *et al.* reported that annealing  $\text{Ti}_3\text{C}_2\text{T}_x$  in argon promoted the formation of a thin, protective  $\text{TiO}_2$  layer on the nanosheet surface. This oxide barrier, particularly effective in densely stacked films, restricted water penetration and preserved the internal structure. Compared to untreated  $\text{Ti}_3\text{C}_2\text{T}_x$ , the annealed films exhibited remarkable stability, maintaining their structure for over ten months in aqueous environments, thereby significantly expanding their potential in practical applications.<sup>70</sup>

In addition to thermal treatments, storage protocols play a crucial role in maintaining the integrity of MXenes. Studies have shown that both the temperature and atmospheric composition directly affect their chemical stability. Zhang *et al.* recommended extending the lifetime of MXene dispersions by storing concentrated nanosheet suspensions with large lateral sizes in sealed, argon-filled containers at low temperatures.<sup>71</sup> Other studies further highlighted that excluding dioxygen and refrigerating dispersions help to minimize oxidative degradation. The solvent medium also influences stability: Maleski *et al.* compared  $\text{Ti}_3\text{C}_2\text{T}_x$  dispersions in 12 different solvents and found that polar organic solvents such as *N,N*-dimethylformamide (DMF), *N*-methyl-2-pyrrolidone (NMP), and propylene carbonate (PC), and ethanol significantly reduced oxidation compared to water. Similarly, isolation of MXene powders from aqueous suspensions *via* freeze-drying or vacuum filtration was reported as an effective approach to prevent aqueous-induced degradation. Collectively, these strategies demonstrate that careful optimization of storage conditions is essential for prolonging the MXene lifetime in both solution and solid states.<sup>72</sup>

Chemical modification and antioxidant incorporation represent another major pathway for enhancing MXene stability. Analogous to food preservation methods, antioxidants such as sodium L-ascorbate (NaAsc) have been employed to protect MXene dispersions. Zhao *et al.* showed that NaAsc forms a stabilizing layer around  $\text{Ti}_3\text{C}_2\text{T}_x$  nanosheets, effectively inhibiting oxidation and maintaining their structure and conductivity for up to three weeks at room temperature.<sup>73</sup> Similarly, Natu *et al.* demonstrated that adding polyanionic salts (polyphosphates, polyborates, and polysilicates) at low concentrations can suppress oxidation initiated at nanosheet edges by creating a protective electrostatic barrier.<sup>74</sup> Beyond antioxidants, functionalization with silanes,<sup>75</sup> polymer coatings<sup>76</sup> and biomolecules such as silk fibroin<sup>77</sup> has been shown to improve hydrophobicity, enhance interfacial interactions, and provide protective encapsulation against oxidative attack. Furthermore, nanoscale carbon coatings offer an effective route



to stabilize MXenes during synthesis. Overall, surface functionalization strategies including antioxidants, polymers, proteins, and carbon coatings provide versatile and effective means to suppress oxidation while retaining the functional properties of MXenes, thereby extending their performance in electrochemical and other applications.

On combining these approaches, process enhancement, solvent choice, antioxidant addition, thermal passivation and encapsulation dramatically extend the lifespan of MXene materials and help retain their electronic and structural properties. These advances pave the way for integration of MXenes into real-world SPECS devices, enabling high efficiency, durable self-powered sensing in applications ranging from environmental monitoring to wearable diagnostics.

## 7. Conclusions

Self-powered electrochemical sensors (SPECSs) offer a transformative solution by integrating energy generation with analyte detection, in which the output energy is in direct relation with the analyte concentrations, paving the way for next-generation devices. The successful realization of high-performance SPECSs relies on advanced materials which are capable of efficiently supporting in both energy conversion and analyte recognition. Among the emerging candidates, 2D MXenes have garnered substantial attention and demonstrated remarkable potential for enabling diverse and highly effective SPECS platforms. This review discusses about the role of MXenes in various self-powered electrochemical sensors such as EBFCs, MFCs and BPECs. The unique combination of properties inherent to MXenes such as metallic conductivity and 2D structure can enhance the charge transfer kinetics and charge separation efficiency, which are vital for maximizing the output signal in self-powered sensors. In addition, the large surface area and functionalized surface of MXenes make them a superior scaffold for immobilizing a wide range of active components including enzymes, aptamers, *etc.* Furthermore, the surface of MXene can act as a template for the *in situ* growth of other functional materials, which can create heterojunctions with improved photocurrents and photoelectric conversion efficiencies. The high electrochemical capacitance of certain MXenes can be used to deliver large instantaneous currents for effectively amplifying the sensitivity of self-powered electrochemical sensors.

The future trajectory for MXene-based SPECSs is exceptionally bright, contingent upon addressing the current limitations. The challenges of long-term operational stability and degradation (Section 5) can be overcome by focusing future research on precise surface engineering and the rational design of novel heterostructures (Section 7). To combat the issue of reproducible, scalable, and cost-effective synthesis (Section 5), future efforts should be directed toward scalable micro-/nanofabrication techniques for device miniaturization (Section 7). Furthermore, the limited understanding of charge transfer mechanisms and the integration of multiple components into miniaturized, robust devices (Section 5) necessitate a deeper fundamental investigation into these systems to unlock the full potential of MXenes for creating transformative autonomous sensing devices. By explicitly addressing these

limitations through concerted research and development efforts, the field can transition from laboratory successes to impactful real-world applications.

## 8. Limitations and future prospects

Despite the rapid progress and demonstrated potential, several challenges impede the widespread practical application of MXenes in self-powered electrochemical sensors. Ensuring long-term operational stability of MXenes and resistance to degradation or oxidation, particularly in complex biological or environmental media will be a critical concern. The synthesis procedures should be modified to get reproducible, scalable, and cost-effective MXenes with precisely controlled properties, which are highly needed for commercial viability. The ongoing research should focus on precise surface engineering of MXenes to tailor functional groups towards achieving specific recognition and on the rational design of novel heterostructures for getting the maximum synergistic effects. To enable testing and validation of MXene-based SPECSs at higher TRLs, future work must focus on stabilising MXenes with antioxidants, polymers, proteins, and carbon coatings. These strategies will help suppress oxidation related degradation of the MXene layer, thus helping long-term anchoring of bioreceptors and maintaining the performance characteristics of the SPECSs. Another key research direction in the same vein involves not only tailoring MXenes with functional groups for biorecognition element immobilisation but also developing methods to synthesize MXene-molecularly imprinted polymer (MIP) composites. This strategy will help bypass limitations associated with conventional bioreceptors like aptamers and antibodies while exhibiting the same specificity. A synergy between enzyme driven power production and MXene-MIP composite-based sensing is a promising approach in this direction.

Towards improving energy conversion efficiencies, MXene integrated energy storage systems with better power management and exploring hybrid energy harvesting modes along with advancing scalable micro-/nanofabrication techniques for device miniaturization need to be considered. For rational design optimization of MXene-based systems, a deeper fundamental understanding of charge transfer mechanisms and synergistic effects in complex MXene-based systems should be thoroughly investigated. Moreover, the effective energy management solutions should be applied for certain high-demand applications, and the significant engineering challenges in the integration of multiple components into miniaturized, robust devices need to be solved.

Further exploration could involve MFCs, which have been realized using diverse electrode materials and are being considered for wearable and environmental sensing.<sup>78–81</sup> Given that MXenes have already demonstrated success in MFC device realization, attributable to their high electrical conductivity, large active surface area, inherent biocompatibility, and ability to facilitate efficient extracellular electron transfer (EET), the focused application of MXene-based MFCs for self-powered wearable and environmental sensing presents a compelling, yet relatively underexplored, research avenue.<sup>82–84</sup> Future



reports could specifically address this niche, bridging the gap in leveraging these advanced MXene–MFC systems for such targeted sensing applications. Similarly, a parallel research thrust could explore applications of MXenes in self-powered devices integrating photosynthetic systems. This could involve employing isolated photosynthetic receptors (like thylakoids),<sup>85</sup> or whole microorganisms,<sup>86</sup> such as algae,<sup>87</sup> phytoplankton,<sup>88</sup> and potentially engineered yeast strains, thereby opening further avenues for novel bio-hybrid sensor development—an area also warranting deeper future investigation, including the potential role of MXenes in enhancing such photosynthetic bio-interfaces.

Nevertheless, the future trajectory for MXene-based SPECSs is exceptionally bright for translating laboratory successes into impactful real-world applications. By addressing the current limitations through these concerted research and development efforts, the field of MXene-based SPECSs can unlock the full potential of MXenes to create truly transformative autonomous sensing devices for diverse applications.

## Author contributions

Conceptualization—AMA and PAR; supervision—PAR and SS; validation—AMA, SS, and PAR; writing – original draft—AMA, MM, and MA; writing – review & editing—AMA, SS, and PAR.

## Conflicts of interest

There are no conflicts to declare.

## Data availability

This manuscript is a review article that compiles, interprets, and discusses findings from previously published, peer-reviewed studies in reputable scientific journals. All data, results, and figures presented here are drawn directly from these original sources. Permissions have been secured for the reproduction of figures and any other materials, and full citations and acknowledgments are provided to appropriately credit the original authors and publications. No new primary data were produced or analyzed for this work. Additional details regarding sources or permissions for reproduced content can be obtained from the corresponding author upon request.

## Acknowledgements

PAR acknowledges the Ramalingaswami fellowship (BT/RLF/Re-entry/75/2020) from the Department of Biotechnology (DBT), Government of India. The authors acknowledge the Indian Institute of Technology Palakkad for providing the research funding.

## References

- 1 H. Zeng, K. Liang, L. Jiang, D. Zhao and B. Kong, Electrochemical Sensing Mechanisms and Interfacial Design Strategies of Mesoporous Nanochannel Membranes

- in Biosensing Applications, *Acc. Chem. Res.*, 2025, **58**(5), 732–745, DOI: [10.1021/acs.accounts.4c00764](https://doi.org/10.1021/acs.accounts.4c00764).
- 2 M. Grattieri and S. D. Minter, Self-Powered Biosensors, *ACS Sens.*, 2018, **3**(1), 44–53, DOI: [10.1021/acssensors.7b00818](https://doi.org/10.1021/acssensors.7b00818).
- 3 F. J. del Campo, Self-powered electrochemical sensors, *Curr. Opin. Electrochem.*, 2023, **41**, 101356, DOI: [10.1016/j.coelec.2023.101356](https://doi.org/10.1016/j.coelec.2023.101356).
- 4 S. K. Sailapu and C. Menon, Engineering Self-Powered Electrochemical Sensors Using Analyzed Liquid Sample as the Sole Energy Source, *Adv. Sci.*, 2022, **9**(29), 2203690, DOI: [10.1002/advs.202203690](https://doi.org/10.1002/advs.202203690).
- 5 X. Qu, X. Liu, Y. Yue, Y. Tang and P. Miao, Triboelectric nanogenerator-enabled self-powered strategies for sensing applications, *TrAC, Trends Anal. Chem.*, 2025, **185**, 118191, DOI: [10.1016/j.trac.2025.118191](https://doi.org/10.1016/j.trac.2025.118191).
- 6 M. Li, J. Chen, W. Zhong, M. Luo, W. Wang, X. Qing, Y. Lu, Q. Liu, K. Liu, Y. Wang and D. Wang, Large-Area, Wearable, Self-Powered Pressure–Temperature Sensor Based on 3D Thermoelectric Spacer Fabric, *ACS Sens.*, 2020, **5**(8), 2545–2554, DOI: [10.1021/acssensors.0c00870](https://doi.org/10.1021/acssensors.0c00870).
- 7 P. Yang, X. Hou, X. Gao, Y. Peng, Q. Li, Q. Niu and Q. Liu, Recent Trends in Self-Powered Photoelectrochemical Sensors: From the Perspective of Signal Output, *ACS Sens.*, 2024, **9**(2), 577–588, DOI: [10.1021/acssensors.3c02198](https://doi.org/10.1021/acssensors.3c02198).
- 8 M. A. M. Hasan, H. Wu and Y. Yang, Redox-induced electricity for energy scavenging and self-powered sensors, *J. Mater. Chem. A*, 2021, **9**(35), 19116–19148, DOI: [10.1039/D1TA02287C](https://doi.org/10.1039/D1TA02287C).
- 9 W. Ou-Yang, L. Liu, M. Xie, S. Zhou, X. Hu, H. Wu, Z. Tian, X. Chen, Y. Zhu and J. Li, Recent advances in triboelectric nanogenerator-based self-powered sensors for monitoring human body signals, *Nano Energy*, 2024, **120**, 109151, DOI: [10.1016/j.nanoen.2023.109151](https://doi.org/10.1016/j.nanoen.2023.109151).
- 10 X. Xiao, H.-q. Xia, R. Wu, L. Bai, L. Yan, E. Magner, S. Cosnier, E. Lojou, Z. Zhu and A. Liu, Tackling the Challenges of Enzymatic (Bio)Fuel Cells, *Chem. Rev.*, 2019, **119**(16), 9509–9558, DOI: [10.1021/acs.chemrev.9b00115](https://doi.org/10.1021/acs.chemrev.9b00115).
- 11 M. Doglioni, M. Nardello and D. Brunelli, Plant Microbial Fuel Cells: Energy Sources and Biosensors for battery-Free Smart Agriculture, *IEEE Transactions on AgriFood Electronics*, 2024, **2**(2), 460–470, DOI: [10.1109/TAFE.2024.3417644](https://doi.org/10.1109/TAFE.2024.3417644).
- 12 J. Zhu, D. Shao, W. Wen, Z. Tian, X. Zhang and S. Wang, Self-powered electrochemical sensor based on photoelectrode: an up-to-date review, *Coord. Chem. Rev.*, 2024, **518**, 216095, DOI: [10.1016/j.ccr.2024.216095](https://doi.org/10.1016/j.ccr.2024.216095).
- 13 G. Li, Z. Li, C. Zhang, C. Xu, X. Zheng and Z. Hu, An integrated bio-photoelectrochemical cell with hundreds of microwatt-level power density for sustainable electricity harvesting, *Chem. Eng. J.*, 2025, **505**, 159485, DOI: [10.1016/j.cej.2025.159485](https://doi.org/10.1016/j.cej.2025.159485).
- 14 H. Zhang, Y. Yu, L. Zhang and S. Dong, Water/oxygen circulation system-based fuel-free bio-photoelectrochemical cells by integrating a Ni: FeOOH/BiVO<sub>4</sub> photoanode, *Angew. Chem., Int. Ed.*, 2018, **130**, 1563–1567, DOI: [10.1002/ange.201710738](https://doi.org/10.1002/ange.201710738).





- 15 P. Bollella, G. Fusco, D. Stevar, L. Gorton, R. Ludwig, S. Ma, H. Boer, A. Koivula, C. Tortolini, G. Favero, *et al.*, A Glucose/Oxygen Enzymatic Fuel Cell based on Gold Nanoparticles modified Graphene Screen-Printed Electrode. Proof-of-Concept in Human Saliva, *Sens. Actuators, B*, 2018, **256**, 921–930, DOI: [10.1016/j.snb.2017.10.025](https://doi.org/10.1016/j.snb.2017.10.025).
- 16 K. P. Prasad, Y. Chen and P. Chen, Three-Dimensional Graphene-Carbon Nanotube Hybrid for High-Performance Enzymatic Biofuel Cells, *ACS Appl. Mater. Interfaces*, 2014, **6**(5), 3387–3393, DOI: [10.1021/am405432b](https://doi.org/10.1021/am405432b).
- 17 F. Shen, D. Pankratov, A. Halder, X. Xiao, M. D. Toscano, J. Zhang, J. Ulstrup, L. Gorton and Q. Chi, Two-dimensional graphene paper supported flexible enzymatic fuel cells, *Nanoscale Adv.*, 2019, **1**(7), 2562–2570, DOI: [10.1039/C9NA00178F](https://doi.org/10.1039/C9NA00178F).
- 18 C. H. Kwon, Y. Ko, D. Shin, M. Kwon, J. Park, W. K. Bae, S. W. Lee and J. Cho, High-power hybrid biofuel cells using layer-by-layer assembled glucose oxidase-coated metallic cotton fibers, *Nat. Commun.*, 2018, **9**(1), 4479, DOI: [10.1038/s41467-018-06994-5](https://doi.org/10.1038/s41467-018-06994-5).
- 19 J. Cai, F. Shen, J. Zhao and X. Xiao, Enzymatic biofuel cell: a potential power source for self-sustained smart textiles, *iScience*, 2024, **27**(2), 108998, DOI: [10.1016/j.isci.2024.108998](https://doi.org/10.1016/j.isci.2024.108998).
- 20 A. M. Arjun, M. Ankitha, N. Shabana, P. V. Vaishag, F. Shamsheera, M. Mufeeda and P. A. Rasheed, An overview on surface modification of niobium MXenes for diagnostic and prognostic applications, *FlatChem*, 2023, **41**, 100538, DOI: [10.1016/j.flatc.2023.100538](https://doi.org/10.1016/j.flatc.2023.100538).
- 21 O. Salim, K. A. Mahmoud, K. K. Pant and R. K. Joshi, Introduction to MXenes: synthesis and characteristics, *Mater. Today Chem.*, 2019, **14**, 100191, DOI: [10.1016/j.mtchem.2019.08.010](https://doi.org/10.1016/j.mtchem.2019.08.010).
- 22 P. A. Rasheed, R. P. Pandey, F. Banat and S. W. Hasan, Recent advances in niobium MXenes: synthesis, properties, and emerging applications, *Matter*, 2022, **5**(2), 546–572, DOI: [10.1016/j.matt.2021.12.021](https://doi.org/10.1016/j.matt.2021.12.021).
- 23 M. P. Bilbana, Electrochemical properties of MXenes and applications, *Adv. Sens. Energy Mater.*, 2023, **2**(4), 100080, DOI: [10.1016/j.asems.2023.100080](https://doi.org/10.1016/j.asems.2023.100080).
- 24 M. Mim, K. Habib, S. N. Farabi, S. A. Ali, M. A. Zaed, M. Younas and S. Rahman, MXene: A Roadmap to Sustainable Energy Management, Synthesis Routes, Stabilization, and Economic Assessment, *ACS Omega*, 2024, **9**(30), 32350–32393, DOI: [10.1021/acsomega.4c04849](https://doi.org/10.1021/acsomega.4c04849).
- 25 K. C. Chan, X. Guan, T. Zhang, K. Lin, Y. Huang, L. Lei, Y. Georgantas, Y. Gogotsi, M. A. Bissett and I. A. Kinloch, The fabrication of Ti<sub>3</sub>C<sub>2</sub> and Ti<sub>3</sub>CN MXenes by electrochemical etching, *J. Mater. Chem. A*, 2024, **12**(37), 25165–25175, DOI: [10.1039/D4TA03457K](https://doi.org/10.1039/D4TA03457K).
- 26 D. Wang, C. Zhou, A. S. Filatov, W. Cho, F. Lagunas, M. Wang, S. Vaikuntanathan, C. Liu, R. F. Klie and D. V. Talapin, Direct synthesis and chemical vapor deposition of 2D carbide and nitride MXenes, *Science*, 2023, **379**(6638), 1242–1247, DOI: [10.1126/science.add9204](https://doi.org/10.1126/science.add9204).
- 27 M. Aizudin, M. K. Sudha, R. Goei, S. K. Lua, R. P. Pottammel, A. I. Y. Tok and E. H. Ang, Sustainable Production of Molybdenum Carbide (MXene) from Fruit Wastes for Improved Solar Evaporation, *Chem.–Eur. J.*, 2023, **29**(2), e202203184, DOI: [10.1002/chem.202203184](https://doi.org/10.1002/chem.202203184).
- 28 M. Mozafari and M. Soroush, Surface functionalization of MXenes, *Mater. Adv.*, 2021, **2**(22), 7277–7307, DOI: [10.1039/D1MA00625H](https://doi.org/10.1039/D1MA00625H).
- 29 T. P. Nguyen, D. M. T. Nguyen, D. L. Tran, H. K. Le, D.-V. N. Vo, S. S. Lam, R. S. Varma, M. Shokouhimehr, C. C. Nguyen and Q. V. Le, MXenes: applications in electrocatalytic, photocatalytic hydrogen evolution reaction and CO<sub>2</sub> reduction, *Mol. Catal.*, 2020, **486**, 110850, DOI: [10.1016/j.mcat.2020.110850](https://doi.org/10.1016/j.mcat.2020.110850).
- 30 C. Tsounis, P. V. Kumar, H. Masood, R. P. Kulkarni, G. S. Gautam, C. R. Müller, R. Amal and D. A. Kuznetsov, Advancing MXene Electrocatalysts for Energy Conversion Reactions: Surface, Stoichiometry, and Stability, *Angew. Chem., Int. Ed.*, 2023, **62**(4), e202210828, DOI: [10.1002/anie.202210828](https://doi.org/10.1002/anie.202210828).
- 31 S. Abdolhosseinzadeh, R. Schneider, M. Jafarpour, C. Merlet, F. Nüesch, C. Zhang and J. Heier, MXene Inks for High-Throughput Printing of Electronics, *Adv. Electron. Mater.*, 2025, **11**(2), 2400170, DOI: [10.1002/aelm.202400170](https://doi.org/10.1002/aelm.202400170).
- 32 E. Quain, T. S. Mathis, N. Kurra, K. Maleski, K. L. Van Aken, M. Alhabeb, H. N. Alshareef and Y. Gogotsi, Direct Writing of Additive-Free MXene-in-Water Ink for Electronics and Energy Storage, *Adv. Mater. Technol.*, 2019, **4**(1), 1800256, DOI: [10.1002/admt.201800256](https://doi.org/10.1002/admt.201800256).
- 33 L. Xu, T. Wu, P. R. C. Kent and D. e. Jiang, Interfacial charge transfer and interaction in the MXene/TiO<sub>2</sub> heterostructures, *Phys. Rev. Mater.*, 2021, **5**(5), 054007, DOI: [10.1103/PhysRevMaterials.5.054007](https://doi.org/10.1103/PhysRevMaterials.5.054007).
- 34 S. Zhou, X. Yang, W. Pei, N. Liu and J. Zhao, Heterostructures of MXenes and N-doped graphene as highly active bifunctional electrocatalysts, *Nanoscale*, 2018, **10**(23), 10876–10883, DOI: [10.1039/C8NR01090K](https://doi.org/10.1039/C8NR01090K).
- 35 Y. Tan, L. Yang, D. Zhai, L. Sun, S. Zhai, W. Zhou, X. Wang, W.-Q. Deng and H. Wu, MXene-Derived Metal-Organic Framework@MXene Heterostructures toward Electrochemical NO Sensing, *Small*, 2022, **18**(50), 2204942, DOI: [10.1002/smll.202204942](https://doi.org/10.1002/smll.202204942).
- 36 K. Ji, Z. Liang, P. Wang, Z. Li, Q. Ma and X. Su, Mxene-based capacitive enzyme-free biofuel cell self-powered sensor for lead ion detection in human plasma, *Chem. Eng. J.*, 2024, **495**, 153598, DOI: [10.1016/j.cej.2024.153598](https://doi.org/10.1016/j.cej.2024.153598).
- 37 S. Sun, M. Su, H. Xiao, X. Yin, Y. Liu, W. Yang and Y. Chen, Self-powered biosensing platform for highly sensitive detection of soluble CD44 protein, *Talanta*, 2024, **272**, 125824, DOI: [10.1016/j.talanta.2024.125824](https://doi.org/10.1016/j.talanta.2024.125824).
- 38 K. Ji, P. Wang, Y. Li, Q. Ma and X. Su, Ti<sub>3</sub>C<sub>2</sub>Tx/Au NPs/PPy ternary heterostructure-based intra-capacitive self-powered sensor for DEHP detection, *J. Hazard. Mater.*, 2025, **488**, 137311, DOI: [10.1016/j.jhazmat.2025.137311](https://doi.org/10.1016/j.jhazmat.2025.137311).
- 39 D. Xiao, M. Zou and M. Huang, Wearable self-powered electrochemical sensor with MXene/PU composite and advanced electrodes for non-invasive lactate detection during physical activity, *Mater. Sci. Eng., B*, 2025, **322**, 118647, DOI: [10.1016/j.mseb.2025.118647](https://doi.org/10.1016/j.mseb.2025.118647).



- 40 Z. Qiu, X. Xue, Y. Lei, X. Lin, D. Tang and Y. Chen, MXene-TiO<sub>2</sub>-based photocatalytic fuel cell with bioresponsive controlled glucose release system: an innovative mode for ochratoxin A detection, *Anal. Chim. Acta*, 2023, **1257**, 341126, DOI: [10.1016/j.aca.2023.341126](https://doi.org/10.1016/j.aca.2023.341126).
- 41 Y. Jin, Y. Luan, Z. Wu, W. Wen, X. Zhang and S. Wang, Photocatalytic Fuel Cell-Assisted Molecularly Imprinted Self-Powered Sensor: A Flexible and Sensitive Tool for Detecting Aflatoxin B1, *Anal. Chem.*, 2021, **93**(39), 13204–13211, DOI: [10.1021/acs.analchem.1c02074](https://doi.org/10.1021/acs.analchem.1c02074).
- 42 J. Sun, R. Zhu, X. Du, B. Zhang, M. Zheng, X. Ji and L. Geng, An ultrasensitive photo-driven self-powered aptasensor for microcystin-RR assay based on ZnIn<sub>2</sub>S<sub>4</sub>/Ti<sub>3</sub>C<sub>2</sub> MXenes integrated with a matching capacitor for multiple signal amplification, *Analyst*, 2023, **148**(20), 5060–5069, DOI: [10.1039/D3AN00914A](https://doi.org/10.1039/D3AN00914A).
- 43 X. Ji, X. Du, J. Sun, B. Zhang, Y. Lian, M. Zheng, R. Zhu and L. Geng, Persulfate mediated single-channel bimodal self-checking light-assisted self-powered aptasensor for highly accurate assay, *Sens. Actuators, B*, 2023, **397**, 134647, DOI: [10.1016/j.snb.2023.134647](https://doi.org/10.1016/j.snb.2023.134647).
- 44 J. Zhu, Y. Wang, Z. Wu, Z. Wu, W. Wen, X. Zhang and S. Wang, Self-powered electrochemical sensing platform based on zinc-air battery via synergy of the light filtering effect and photoassisted oxygen reduction reaction, *Sens. Actuators, B*, 2022, **355**, 131320, DOI: [10.1016/j.snb.2021.131320](https://doi.org/10.1016/j.snb.2021.131320).
- 45 F. E. Ab Latif, A. Numan, N. M. Mubarak, M. Khalid, E. C. Abdullah, N. A. Manaf and R. Walvekar, Evolution of MXene and its 2D heterostructure in electrochemical sensor applications, *Coord. Chem. Rev.*, 2022, **471**, 214755, DOI: [10.1016/j.ccr.2022.214755](https://doi.org/10.1016/j.ccr.2022.214755).
- 46 J. Liu, Z. Tao, Y. Zhang, T. Ni, B. Liu and Z. Zhang, Dual-modal flexible zinc-air battery-driven self-powered and impedimetric aptasensor based on the hybrid of V<sub>2</sub>CTx MXene and bimetallic layered double hydroxide for the detection of cortisol, *Microchem. J.*, 2024, **197**, 109757, DOI: [10.1016/j.microc.2023.109757](https://doi.org/10.1016/j.microc.2023.109757).
- 47 J. Liu, M. Wang, Z. Tao, L. He, C. Guo, B. Liu and Z. Zhang, Photo-assisted Zn-air battery-driven self-powered aptasensor based on the 2D/2D Schottky heterojunction of cadmium-doped molybdenum disulfide and Ti<sub>3</sub>C<sub>2</sub>Tx nanosheets for the sensitive detection of penicillin G, *Anal. Chim. Acta*, 2023, **1270**, 341396, DOI: [10.1016/j.aca.2023.341396](https://doi.org/10.1016/j.aca.2023.341396).
- 48 L. Zhou, D. Liu, L. Liu, L. He, X. Cao, J. Wang and Z. L. Wang, Recent Advances in Self-Powered Electrochemical Systems, *Research*, 2021, **2021**, 4673028, DOI: [10.34133/2021/4673028](https://doi.org/10.34133/2021/4673028).
- 49 V. Galstyan, I. D'Onofrio, A. Liboà, G. De Giorgio, D. Vurro, L. Rovati, G. Tarabella and P. D'Angelo, Recent Advances in Self-Powered Electrochemical Biosensors for Early Diagnosis of Diseases, *Adv. Mater. Technol.*, 2024, **9**(21), 2400395, DOI: [10.1002/admt.202400395](https://doi.org/10.1002/admt.202400395).
- 50 C. Liu, Z. Feng, T. Yin, T. Wan, P. Guan, M. Li, L. Hu, C.-H. Lin, Z. Han, H. Xu, *et al.*, Multi-Interface Engineering of MXenes for Self-Powered Wearable Devices, *Adv. Mater.*, 2024, **36**(42), 2403791, DOI: [10.1002/adma.202403791](https://doi.org/10.1002/adma.202403791).
- 51 Z. Zequan, C. Xia and W. Ning, Beyond energy harvesting: a review on the critical role of MXene in triboelectric nanogenerator, *Energy Mater.*, 2024, **4**(3), 400035, DOI: [10.20517/energymater.2023.121](https://doi.org/10.20517/energymater.2023.121).
- 52 L. Manjakkal, L. Yin, A. Nathan, J. Wang and R. Dahiya, Energy Autonomous Sweat-Based Wearable Systems, *Adv. Mater.*, 2021, **33**(35), 2100899, DOI: [10.1002/adma.202100899](https://doi.org/10.1002/adma.202100899).
- 53 L. Yin, K. N. Kim, J. Lv, F. Tehrani, M. Lin, Z. Lin, J.-M. Moon, J. Ma, J. Yu, S. Xu and J. Wang, A self-sustainable wearable multi-modular E-textile bioenergy microgrid system, *Nat. Commun.*, 2021, **12**(1), 1542, DOI: [10.1038/s41467-021-21701-7](https://doi.org/10.1038/s41467-021-21701-7).
- 54 L. Yin, J.-M. Moon, J. R. Sempionatto, M. Lin, M. Cao, A. Trifonov, F. Zhang, Z. Lou, J.-M. Jeong, S.-J. Lee, *et al.*, A passive perspiration biofuel cell: high energy return on investment, *Joule*, 2021, **5**(7), 1888–1904, DOI: [10.1016/j.joule.2021.06.004](https://doi.org/10.1016/j.joule.2021.06.004).
- 55 C. Ye, M. Wang, J. Min, R. Y. Tay, H. Lukas, J. R. Sempionatto, J. Li, C. Xu and W. Gao, A wearable aptamer nanobiosensor for non-invasive female hormone monitoring, *Nat. Nanotechnol.*, 2023, **19**, 330–337, DOI: [10.1038/s41565-023-01513-0](https://doi.org/10.1038/s41565-023-01513-0).
- 56 Á. Torrinha, M. Tavares, C. Delerue-Matos and S. Morais, A self-powered biosensor for glucose detection using modified pencil graphite electrodes as transducers, *Chem. Eng. J.*, 2021, **426**, 131835, DOI: [10.1016/j.cej.2021.131835](https://doi.org/10.1016/j.cej.2021.131835).
- 57 J. Xu, Y.-H. Wang, Z. Wei, F.-T. Wang and K.-J. Huang, Significantly improving the performance of self-powered biosensor by effectively combining with high-energy enzyme biofuel cells, N-doped graphene, and ultrathin hollow carbon shell, *Sens. Actuators, B*, 2021, **327**, 128933, DOI: [10.1016/j.snb.2020.128933](https://doi.org/10.1016/j.snb.2020.128933).
- 58 Y. Ma, J. Shi, Y. Lin, Y. Wu, H. Luo, J. Yan, K.-J. Huang and X. Tan, Smart enzyme-free amplification dual-mode self-powered platform designed on two-dimensional networked graphdiyne and DNA nanorods for ultra-sensitive detection of breast cancer biomarkers, *Anal. Chim. Acta*, 2023, **1280**, 341876, DOI: [10.1016/j.aca.2023.341876](https://doi.org/10.1016/j.aca.2023.341876).
- 59 W. Yang, J. Ke, Z. Xiao, Z. Song, X. Chen and Q. Wang, A novel electrocatalytic current dominated self-powered photoelectrochemical sensor based on patterned bipolar electrode, *Anal. Chim. Acta*, 2025, **1361**, 344157, DOI: [10.1016/j.aca.2025.344157](https://doi.org/10.1016/j.aca.2025.344157).
- 60 M. Ashton, K. Mathew, R. G. Hennig and S. B. Sinnott, Predicted surface composition and thermodynamic stability of MXenes in solution, *J. Phys. Chem. C*, 2016, **120**(6), 3550–3556, DOI: [10.1021/acs.jpcc.5b11887](https://doi.org/10.1021/acs.jpcc.5b11887).
- 61 M. Seredych, C. E. Shuck, D. Pinto, M. Alhabeb, E. Precetti, G. Deysher, B. Anasori, N. Kurra and Y. Gogotsi, High-temperature behavior and surface chemistry of carbide MXenes studied by thermal analysis, *Chem. Mater.*, 2019, **31**(9), 3324–3332, DOI: [10.1021/acs.chemmater.9b00397](https://doi.org/10.1021/acs.chemmater.9b00397).
- 62 C. Zhang, S. J. Kim, M. Ghidui, M.-Q. Zhao, M. W. Barsoum, V. Nicolosi and Y. Gogotsi, Layered Orthorhombic Nb<sub>2</sub>O<sub>5</sub>@Nb<sub>4</sub>C<sub>3</sub>Tx and TiO<sub>2</sub>@Ti<sub>3</sub>C<sub>2</sub>Tx Hierarchical Composites for High Performance Li-ion Batteries, *Adv.*



- Funct. Mater.*, 2016, **26**(23), 4143–4151, DOI: [10.1002/adfm.201600682](#).
- 63 R. B. Rakhi, B. Ahmed, M. N. Hedhili, D. H. Anjum and H. N. Alshareef, Effect of postetch annealing gas composition on the structural and electrochemical properties of Ti<sub>2</sub>CT x MXene electrodes for supercapacitor applications, *Chem. Mater.*, 2015, **27**(15), 5314–5323, DOI: [10.1021/acs.chemmater.5b01623](#).
  - 64 Z. Li, L. Wang, D. Sun, Y. Zhang, B. Liu, Q. Hu and A. Zhou, Synthesis and thermal stability of two-dimensional carbide MXene Ti<sub>3</sub>C<sub>2</sub>, *Mater. Sci. Eng., B*, 2015, **191**, 33–40, DOI: [10.1016/j.mseb.2014.10.009](#).
  - 65 R. Thakur, A. VahidMohammadi, J. Moncada, W. R. Adams, M. Chi, B. Tatarchuk, M. Beidaghi and C. A. Carrero, Insights into the thermal and chemical stability of multilayered V<sub>2</sub>CT x MXene, *Nanoscale*, 2019, **11**(22), 10716–10726, DOI: [10.1039/C9NR03020D](#).
  - 66 T. Habib, X. Zhao, S. A. Shah, Y. Chen, W. Sun, H. An, J. L. Lutkenhaus, M. Radovic and M. J. Green, Oxidation stability of Ti<sub>3</sub>C<sub>2</sub>Tx MXene nanosheets in solvents and composite films, *npj 2D Mater. Appl.*, 2019, **3**(1), 8, DOI: [10.1038/s41699-019-0089-3](#).
  - 67 S. Doo, A. Chae, D. Kim, T. Oh, T. Y. Ko, S. J. Kim, D.-Y. Koh and C. M. Koo, Mechanism and kinetics of oxidation reaction of aqueous Ti<sub>3</sub>C<sub>2</sub>Tx suspensions at different pHs and temperatures, *ACS Appl. Mater. Interfaces*, 2021, **13**(19), 22855–22865, DOI: [10.1021/acsami.1c04663](#).
  - 68 X. Zhao, A. Vashisth, J. W. Blivin, Z. Tan, D. E. Holta, V. Kotasthane, S. A. Shah, T. Habib, S. Liu, M. Lutkenhaus, M. Radovic and J. P. H. Green, nanosheet concentration, and antioxidant affect the oxidation of Ti<sub>3</sub>C<sub>2</sub>Tx and Ti<sub>2</sub>CTx MXene dispersions, *Adv. Mater. Interfaces*, 2020, **7**(20), 2000845, DOI: [10.1002/admi.202000845](#).
  - 69 K. Wang, Y. Zhou, W. Xu, D. Huang, Z. Wang and M. Hong, Fabrication and thermal stability of two-dimensional carbide Ti<sub>3</sub>C<sub>2</sub> nanosheets, *Ceram. Int.*, 2016, **42**(7), 8419–8424, DOI: [10.1016/j.ceramint.2016.02.059](#).
  - 70 X. Zhao, D. E. Holta, Z. Tan, J.-H. Oh, I. J. Echols, M. Anas, H. Cao, J. L. Lutkenhaus, M. Radovic and M. J. Green, Annealed Ti<sub>3</sub>C<sub>2</sub>Tz MXene Films for Oxidation-Resistant Functional Coatings, *ACS Appl. Nano Mater.*, 2020, **3**(11), 10578–10585, DOI: [10.1021/acsanm.0c02473](#).
  - 71 X. Li, X. Yin, M. Han, C. Song, X. Sun, H. Xu, L. Cheng and L. Zhang, A controllable heterogeneous structure and electromagnetic wave absorption properties of Ti<sub>2</sub>CTx MXene, *J. Mater. Chem. C*, 2017, **5**(30), 7621–7628, DOI: [10.1039/C7TC01991B](#).
  - 72 K. Maleski, V. N. Mochalin and Y. Gogotsi, Dispersions of two-dimensional titanium carbide MXene in organic solvents, *Chem. Mater.*, 2017, **29**(4), 1632–1640, DOI: [10.1021/acs.chemmater.6b04830](#).
  - 73 X. Zhao, A. Vashisth, E. Prehn, W. Sun, S. A. Shah, T. Habib, Y. Chen, Z. Tan, J. L. Lutkenhaus, M. Radovic and J. M. Green, Antioxidants unlock shelf-stable Ti<sub>3</sub>C<sub>2</sub>Tx (MXene) nanosheet dispersions, *Matter*, 2019, **1**(2), 513–526, DOI: [10.1016/j.matt.2019.05.020](#).
  - 74 V. Natu, J. L. Hart, M. Sokol, H. Chiang, M. L. Taheri and M. W. Barsoum, Edge capping of 2D-MXene sheets with polyanionic salts to mitigate oxidation in aqueous colloidal suspensions, *Angew. Chem.*, 2019, **131**(36), 12785–12790, DOI: [10.1002/ange.201906138](#).
  - 75 J. Ji, L. Zhao, Y. Shen, S. Liu and Y. Zhang, Covalent stabilization and functionalization of MXene via silylation reactions with improved surface properties, *FlatChem*, 2019, **17**, 100128, DOI: [10.1016/j.flatc.2019.100128](#).
  - 76 L. Gao, C. Li, W. Huang, S. Mei, H. Lin, Q. Ou, Y. Zhang, J. Guo, F. Zhang and S. Xu, MXene/polymer membranes: synthesis, properties, and emerging applications, *Chem. Mater.*, 2020, **32**(5), 1703–1747, DOI: [10.1021/acs.chemmater.9b04408](#).
  - 77 M. C. Krecker, D. Bukharina, C. B. Hatter, Y. Gogotsi and V. V. Tsukruk, Bioencapsulated MXene flakes for enhanced stability and composite precursors, *Adv. Funct. Mater.*, 2020, **30**(43), 2004554, DOI: [10.1002/adfm.202004554](#).
  - 78 J. Ryu, M. Landers and S. Choi, A sweat-activated, wearable microbial fuel cell for long-term, on-demand power generation, *Biosens. Bioelectron.*, 2022, **205**, 114128, DOI: [10.1016/j.bios.2022.114128](#).
  - 79 M. Asghary, J. B. Raoof, M. Rahimnejad and R. Ojani, A novel self-powered and sensitive label-free DNA biosensor in microbial fuel cell, *Biosens. Bioelectron.*, 2016, **82**, 173–176, DOI: [10.1016/j.bios.2016.04.023](#).
  - 80 W. Liu, L. Yin, Q. Jin, Y. Zhu, J. Zhao, L. Zheng, Z. Zhou and B. Zhu, Sensing performance of a self-powered electrochemical sensor for H<sub>2</sub>O<sub>2</sub> detection based on microbial fuel cell, *J. Electroanal. Chem.*, 2019, **832**, 97–104, DOI: [10.1016/j.jelechem.2018.10.045](#).
  - 81 Q. Yang, Y. Liu, Z. Li, Z. Yang, X. Wang and Z. L. Wang, Self-Powered Ultrasensitive Nanowire Photodetector Driven by a Hybridized Microbial Fuel Cell, *Angew. Chem., Int. Ed.*, 2012, **51**(26), 6443–6446, DOI: [10.1002/anie.201202008](#).
  - 82 P. D. Kolubah, H. O. Mohamed, M. Ayach, A. R. Hari, H. N. Alshareef, P. Saikaly, K.-J. Chae and P. Castaño, W<sub>2</sub>N-MXene composite anode catalyst for efficient microbial fuel cells using domestic wastewater, *Chem. Eng. J.*, 2023, **461**, 141821, DOI: [10.1016/j.cej.2023.141821](#).
  - 83 X. Hu, J. Qin, Y. Wang, J. Wang, A. Yang, Y. F. Tsang and B. Liu, Synergic degradation chloramphenicol in photo-electrocatalytic microbial fuel cell over Ni/MXene photocathode, *J. Colloid Interface Sci.*, 2022, **628**, 327–337, DOI: [10.1016/j.jcis.2022.08.040](#).
  - 84 K. Gunaseelan, P. S. Rajput, R. Rajumon, M. Ankitha, P. A. Rasheed and P. Gangadharan, A novel MXene coated liquid crystal display anode derived from a futile computer monitor for microbial fuel cell application, *J. Power Sources*, 2024, **609**, 234714, DOI: [10.1016/j.jpowsour.2024.234714](#).
  - 85 K. B. Lam, E. F. Irwin, K. E. Healy and L. Lin, Bioelectrocatalytic self-assembled thylakoids for micro-power and sensing applications, *Sens. Actuators, B*, 2006, **117**(2), 480–487, DOI: [10.1016/j.snb.2005.12.057](#).
  - 86 J. H. Franco, P. Stufano, R. Labarile, D. Lacalamita, P. Lasala, E. Fanizza, M. Trotta, G. M. Farinola and M. Grattieri, Intact





- photosynthetic bacteria-based electrodes for self-powered metal ions monitoring, *Biosens. Bioelectron.*, 2024, **21**, 100552, DOI: [10.1016/j.biosx.2024.100552](https://doi.org/10.1016/j.biosx.2024.100552).
- 87 A. Chatterjee, A. Shyam, T. G. Manivasagam and S. K. Batabyal, Spirulina-Based Self-Powered Biological UV Photodetectors, *ACS Appl. Electron. Mater.*, 2025, **7**(8), 3274–3284, DOI: [10.1021/acsaelm.4c02295](https://doi.org/10.1021/acsaelm.4c02295).
- 88 M. Yang and R. G. Compton, Electrochemical sensors for phytoplankton and ocean health, *Curr. Opin. Electrochem.*, 2023, **42**, 101413, DOI: [10.1016/j.coelec.2023.101413](https://doi.org/10.1016/j.coelec.2023.101413).

